TRIBOLOGICAL STUDIES AND ANALYSIS ON PISTON OF HERMETICALLY SEALED COMPRESSOR

A PROJECT REPORT

SUBMITTED IN PARTIAL FULFILLMENT OF THE REQUIREMENTS

FOR THE AWARD OF THE DEGREE

OF

MASTER OF TECHNOLOGY

IN

COMPUTATIONAL DESIGN

Submitted by:

ALI IRSHAD

(2K17/CDN/01)

Under the supervision of

Prof. R. C. SINGH   **Prof. RANGANATH M. SINGARI**

Prof. Mechanical Department   Head of Department of Design

DEPARTMENT OF MECHANICAL ENGINEERING

DELHI TECHNOLOGICAL UNIVERSITY

(Formerly Delhi College of Engineering)

Bawana Road, Delhi-110042

JULY, 2019

DEPARTMENT OF MECHANICAL ENGINEERING,

DELHI TECHNOLOGICAL UNIVERSITY

(Formerly Delhi College of Engineering)

Bawana Road, New Delhi -110042

<u>**CANDIDATE'S DECLARATION**</u>

I, ALI IRSHAD, Roll No. - 2K17/CDN/01 student of M.Tech (Computational Design), hereby declare that the project dissertation titled 'Tribological analysis on hermetically sealed compressor' which is submitted by us to the Department of Mechanical Engineering, Delhi Technological University, Delhi in partial fulfillment of the requirement for the award of the degree of Master of Technology, is original and not copied from any source without proper citation. This work has not previously formed the basis for the award of any degree, diploma associate ship, fellowship or other similar title or recognition.

Place: New Delhi   **Ali Irshad**

Date: (**2K17/CDN/01**)

DEPARTMENT OF MECHANICAL ENGINEERING,

DELHI TECHNOLOGICAL UNIVERSITY

(Formerly Delhi College of Engineering)

Bawana Road, New Delhi -110042

CERTIFICATE

I hereby certify that the Project Dissertation titled "Tribological analysis on hermetically sealed compressor" which was submitted by Ali Irshad, Roll No. - 2K17/CDN/01 Department of Mechanical Engineering, Delhi Technological University, New Delhi in partial fulfillment of the requirement for the award of the degree of Master of Technology, is a record of the project carried out by the student under my supervision. To the best of my knowledge this work has not been submitted in part or full for any Degree or Diploma in this University or elsewhere.

Prof. R. C. Singh   **Prof. Ranganath M. Singari**

SUPERVISOR   **SUPERVISOR**

Professor   Professor

Deptt. Of Mechanical Engineering   Deptt. Of Mechanical Engineering

Delhi Technological University   Delhi Technological University

Date: Place: New Delhi

ACKNOWLEDGEMENT

The efficient and effective completion of the project is unfinished without giving the acknowledgement to everyone who made it feasible and the person whose guidance and support was very crucial.

I owe a lot to my supervisor, Prof. Ranganath M. Singari, Professor, Department of Mechanical Engineering, for supporting and guiding to explore the depth in the search of knowledge and creativity. I would like to thank him for all the assistance and being a source of motivation whenever needed.

I am obliged to everyone who directly or indirectly lent his/her support for successful completion the task. I would like to thank the Department of Mechanical Engineering for providing us advanced computational lab facilities for producing efficient work.

In the end, I thank my parents for always being supportive.

CONTENTS

List of Tables

List of Figures

ABSTRACT

In this project analysis of hermetically sealed compressor is done using linear reciprocating tribometer, the analysis of wear is carried out in the cylinder piston unit of hermetically sealed compressor. Moreover a new material is casted and tested using LRT the results of wear, frictional forces, coefficient of friction is obtained and graph is plotted. The results of the existing material are verified against the newly developed material, and analysis of results been done.

The optical structure of sample is viewed using Scanning Electron Microscope (SEM) technique. The microscopic images shows mixing of grains of different elements. The percentage composition of material is computed using Energy Dispersive X-Ray Spectroscopy (EDAX), the composition is seen over a spectrum (region), peaks of elemental composition is plotted in the form of graph. Tabular representation of data is also done for computational purpose.

The results of wear obtain are the optimized using Taguchi method and the deviation of wear from mean values is noticed. Deviation in wear is computed on parameters like load, time, temperature and graphs of respective are formed against wear. The specimen is then tested for hardness in a hardness tester, the probe of tester is touched at different points and value is computed.

CHAPTER 1: INTRODUCTION

1.1 COMPRESSOR

A compressor is a mechanical device that increases the pressure of gas by reducing the volume. A compressor is similar in working to that of pump but unlike pump, compressor compresses the volume of gas whereas the pump is used to transmit fluid from a place to other places. A gas compressor is simply an air compressor. The main action of compressor is to compress the gas for further actions.

Compressor now a days are available in many different sizes from portable to large ones, from reciprocating compressor to rotating compressor. Since this research work is about reciprocating compressor so let's talk about reciprocating compressor in detail. A reciprocating compressor can be driven by electric motor or can be driven by internal combustion engine. Reciprocating compressor ranges from 5 to 30 HP for smaller application whereas they can go up to 1000 HP for larger application. Discharge pressure for larger compressor can go up to 180MPa. Different applications include multi staged air compressor for effective compressor action. Reciprocating compressor is also used in AC and refrigerating applications.

Reciprocating compressor are used at small sites, house hold works and they provide a power output of less than 0.5 HP. Another variety of reciprocating compressor known as hermetically sealed compressor is used in refrigerators and ACs now a days.

1.2 HERMETICALLY SEALED COMPRESSOR

Hermetically sealed compressor are extensively used for refrigeration as well as air conditioning applications. The size of hermetically sealed compressor is usually small and the power output from them is in the range of about 1/20 and 71/2 HP. The installation and maintenance of hermetically sealed compressor is economical. The hermetically sealed compressors are easy to handle and makes very low noise.

The compressor is enclosed in a hard shell of steel, steel shell consists of reciprocating cylinder piston assembly with motor that drives the shaft of the piston. Hermetically sealed compressor is quite different from old days compressor that includes motor and cylinder piston assembly as different entities and are connected to each other through coupling and belts. The hard shell of steel serves as the protection for the inlet components of compressor.

Hermetically sealed compressor consists of mechanical parts in one section whereas consists electrical parts in other section. One section of the enclosed casing the various parts of the compressor like cylinder, piston, connecting rod and the crankshaft. There are more than two cylinder piston assembly in case of multi compressor. Shaft rotates in electrical section which is coupled to the motor. Motor can be single speed or multi-speed. In hermetically sealed compressors the shaft of motor is coupled with crankshaft of cylinder piston unit. The crankshaft of the hermetically sealed reciprocating compressor is formed by extended shaft of the motor.

The steel shell is manufactured in two parts the lower shell and the upper shell, these two shells are either bolted or welded to form the complete casing for compressor. The bolted shells are easy to open in case of compressor fire due to short-circuiting or any other mechanical damages.

Fig.1.1: Hermetically sealed compressor [source: A. Smith et. al.,]

Externally, the envelope contains suction joints and cooling gases related to evaporator and condenser, respectively. There is also an electrical socket.

The specifications of compressor are written on the label of the compressor which is printed outside the compressor. The label which is printed outside contain the details like manufacturing date, name of manufacturer, speed, working frequency and voltage required for its usage.

There are three connectors in the hermetically sealed compressor, the suction, the discharge and the process. The suction connector sucks the refrigerant from evaporator and then supplies to the compressor for compressing the refrigerant whereas the discharge connector discharge the refrigerant for heat exchanging. The purpose of process connector is to refill the refrigerant in case there is any cooling problem or the existing refrigerant is run out of its refrigerant properties.

The power supply provided shall be suitable for the individual compressor. The start device is responsible for starting the compressor by doing the necessary power to enable startup activation. Once the compressor starts to rotate, power is supplied through the motor to the main winding. A flexible connection is provided to the motor via the power cable.

The piston unit and cylinder contain four distinct elements: block, discharge pipe, elbow shaft and piston. The drain pipe is installed on the block, with an oil pump installed at the bottom of the crankshaft. The piston has a piston rod connected through a piston pin. There are two discharge chambers inside the block and are used to enable the compressed radiator to reach the discharge connector.

A suitable power supply is required for the compressor to work. The power at first is supplied to the starter which stars the compressor after the poles of rotor got fixed the power is then supplied to the motor and now motor drives the crankshaft which is connected to the piston.

The valve unit will use the discharge valve and the suction unit, both mounted on the main valve plate. Valves help to open and close fuse panels during suction and discharge operations. This procedure allows the compacted refrigerant to make its way to the discharge chambers. Finally, the silencer is used to reduce the noise caused by the suction

process. It is installed between the suction connector and the suction side of the pump unit.

Fig.1.2: Cut section of hermetically sealed compressor [source: A. Smith et. al.,]

The crankshaft of the piston is connected to the motor, the rotating action of motor is converted to reciprocating motion of cylinder piston assembly. The motion of piston allowed the refrigerant to get sucked and discharged at every in and out motion of the piston.

The valve unit will use the discharge valve and the suction unit, both mounted on the main valve plate. Valves help to open and close fuse panels during suction and discharge operations. This procedure allows the compacted refrigerant to make its way to the discharge chambers. Finally, the silencer is used to reduce the noise caused by the suction process. It is installed between the suction connector and the suction side of the pump unit.
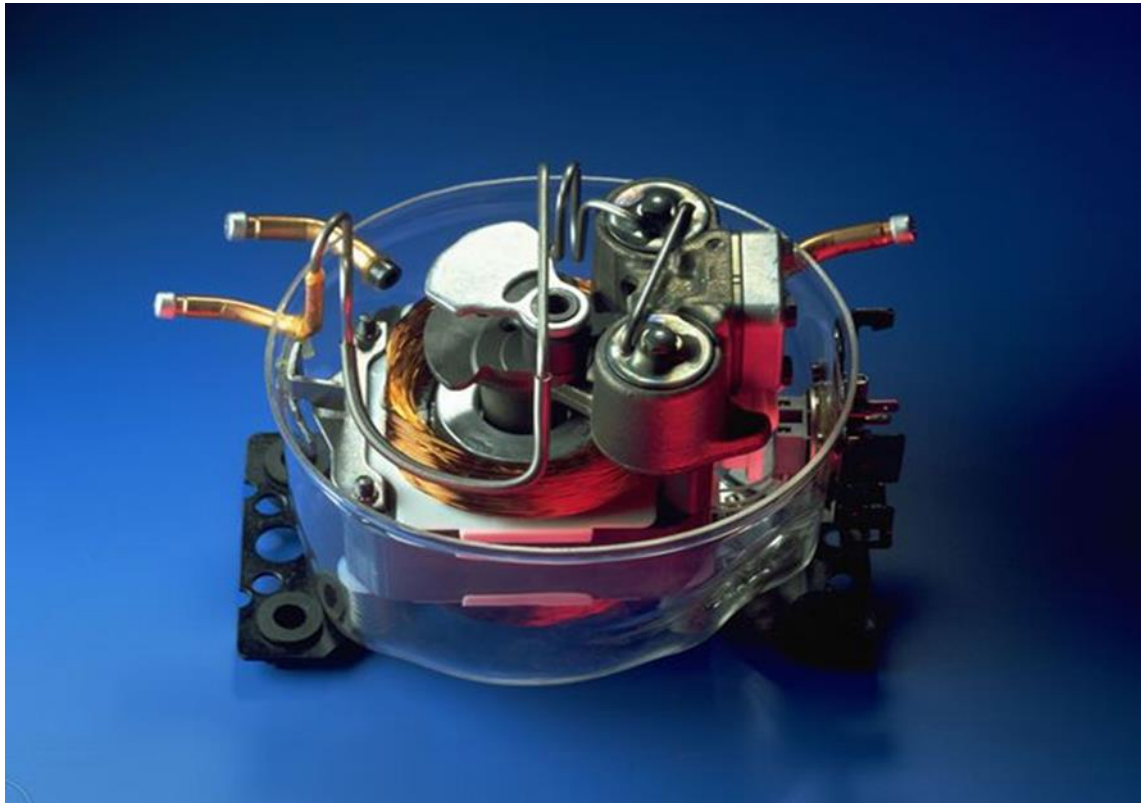
1.3 Parts of hermetically sealed compressor

Fig.1.3: Parts of hermetically sealed compressor [source: N.G. Demas et. al.,]

1. Housing with connectors and baseplates

2. Top covers

3. Blocks with a stator bracket

4. Stators (with screws)

5. Rotors

6. Valve units (screws, cylinder cover, gaskets, valve plate)

7. Crankshafts with grommet

8. Connecting rods with a piston

9. Oil pickup tubes

10. Springs with suspensions

11. Internal discharge tubes (screw, washer, gasket)

The lubricant used in hermetically sealed compressor is R60, it has excellent lubricating properties in extreme temperatures. It's a heavy duty silicone sprayer and also high-performance optical lubricant with high resistance to harsh climatic conditions, temperatures and certain chemical attacks. It is also effective in marine environments to protect against salt spray deposits.

The R60 reduces friction in non-load mechanical assemblies, removes moisture and leaves a residual layer of lubricants to help prevent corrosion. It is widely used as a mold release agent and will not adversely affect rubber and most plastic coatings. Excellent water disposal properties and prevents sticking and binding. Resistant to Weather, sunshine, extreme temperatures and chemical attacks.

CHAPTER 2: LITERATURE REVIEW

2.1 Studies on hermetically sealed compressor

Lusha Tian et al., [1] Thermally treated piston aluminum alloy (Al-13Si-4Cu-2Ni-1Mg-0.25Mn) more age at 350 ° C and 420 ° C respectively, for several times (0-1000 hours). Microstructure of the alloy was reconstructed using optical reconstruction microscope (OM, Nicon300) and electronic microscope transfer (TEM, JEM-2010). Tensile strength at the room was tested and 350 ° C, as well as fatigue bending high cycle of alloy. The results show that Al11Cu5Mn3 nanoparticles are deposited during the high aging process. The size of part formed during aging at 420 ° C higher than those formed at 350 ° C. Both room temperature (RT) and 350 ° C tensile strengths, in addition to the exhausting age of the alloy cycle after re-living at 420 ° C, higher than those of there-lifetime at 350 ° C due to the significant precipitation enhancement effect of Al11Cu5Mn3 nanoparticles.

For different temperatures of aging time, microscope, tensile strength and high cycle fatigue number of alloys changed clearly.

Love kerni et al., [2] This paper focuses on various al alloys used for piston and roller applications and their tribal properties under lubricated conditions. It is important to consider tribal friction characteristics as a major contributor to energy loss. The alloys are used in the manufacture of piston and cylinder due to high thermal conductivity, low density, high strength and excellent castability. The paper discusses various methods adopted to improve friction and corrosion properties aluminum alloy focusing on alloy series used in piston and cylinder applications. Different under the mechanisms of lying leading to improved friction and corrosion properties have also been treated.

Aluminium alloy is a promising material for piston applications and wear because of its good strength to weight Ratio and other critical characteristics of piston application and wear, but poor corrosion resistance is the case that limits their use. One way to improve friction and wear aluminium alloys is the surface structure which allows the

lubricant on the surface under the boundary lubrication conditions. Add some enhancements such as Graphite and carbon fibre in 2xxx series of aluminium alloy, friction and corrosion can be reduced by forming a layer of reinforcement on the surface prevents the metal from touching the metal. Moreover, add solids such as TiB2 in 2024 AA alloy, also lead to improved corrosion resistance. This is due to strong bonding between solids and alloys which prevents the material from being withdrawn from the surface and thus reduces corrosion. Also, add elements such as Si, Mg, and Cu to Al-Si alloys, strength, hardness and abrasion resistance. Alloy can be improved. Heat treatment also improves the hardness and corrosion resistance of alloyed alloys. Adding dual reinforcement molecules in 13 LM alloys, the corrosion resistance has been improved compared to particle enhancement one in the case of LM 13 alloy corrosion resistance and cooling rate is greatly improved by adding iron, manganese. The erosion volume and friction coefficient of the LM 13 alloys decreases with the ceramic phase increase in the alloy due to the reduction in plastic deformation of the alloy by adding fiber.

Zhimin Yao et al., [3] The use of thermal barrier paint (TBCs) is widely used in the industry to provide thermal fatigue protection. For example, in engine design, TBCs are typically observed on combustion chamber components of space engines. In this study, nano-Y2O3 partially stabilized zirconia (PYSZ) was applied to TBC piston to provide protection from heat fatigue of aluminum alloy piston from natural gas engine, to improve the performance of high temperature and convection capacity. This method can eliminate severe restrictions on the development of the natural gas engine and can also be referred to components of other internal combustion engine. Experiments and simulation analyzes were conducted determine the effects of the PYSZ Nano TBCs on temperature distributions and convection. Results showed that the substrate temperature of the PYSZ nano-piston TBCs was much lower (about 16% or 55° C less) than the conventional (uncoated) piston, indicating that TBCs can actually provide protection from thermal fatigue of pistons and reduce thermal damage to compressors. At the same time, the top surface temperature of the piston rose about 52% or 179 ° C after applying the coating, which increased the temperature of the combustion chamber, resulting in improved thermal engine effectiveness.

The result of thermal analysis shows that the natural engine piston subject to high thermal load. Total temperature is relatively high, especially the temperature of the combustion chamber the crown of the piston. The throat saw the room upstairs the temperature, which

was close to the maximum of the piston material, indicating that the throat chamber may potentially undergo overload convection. Thermocouple TBCs analysis results suggest that the highest temperature occurs in ceramic coating, but this the temperature is much lower than the ceramic limit, indicating it works under safe conditions. TBCs coated temperature the substrate is clearly less than the traditional piston substrate, thus coating the TBCs on the piston can effectively reduce the substrate temperature, improve its carrying capacity and higher convection.

W.T. Riad et al., [4] Several aluminium cast pistons used in fuel gas reciprocating compressors suffered from cracking during operation after a short time of service. The pistons were obtained from two manufacturing sources and the failure time was different. Metallurgical investigation was made on the failed pistons to identify the root cause of cracking. The investigation revealed that the cracks primarily existed at the top surfaces of the pistons and joined screwed plugs. The investigation also showed that the cracks had originated as fatigue cracks starting from the roots of broken threads in the body of the pistons. The root cause of failure was found to be the improper screwing of the plugs which resulted in the shear deformation of the threads and development of incipient micro cracks. The difference in failure time was attributed to differences in materials properties and the amount of casting defects. Analysis of the used lube oil showed a significant increase in water content in addition to elements resulting from corrosion of piston parts. These results indicate that appreciable water condensation has occurred in addition to contamination of the lube oil by dust particles and corrosion products. It is known that aluminium components are very sensitive to conditions of dirt in the oil and any foreign matter such as the presence of Fe in oil. Also, the presence of heavy metals in the lubricant has a detrimental effect on the performance of compressor and can cause abrasion and wear to the metallic components of piston-compressor. Water contamination in lubricating oil is known to cause corrosion. The presence of water is known to form hydro sulphuric acid with sulphur present in the form of hydrogen sulphide (H_2S) or other sulphur compounds. Sulphur ingression, in whatever form is usually corrosive to most metals and can result from seal leakage in applications of sour gas compression.

J.D.B. De Mello et al., [5] Friction and wear control can be achieved primarily by considering the nature of the counter faces, together with the environmental conditions. In most cases, a transfer film is found on the sliding surfaces. The environment plays a crucial role on the kinetics of formation and on the composition of the transfer film, and thus strongly influences friction level and wears rates. In this paper, the effect of the actual environment (refrigerant) present in hermetic compressors on the tribological behaviour of a Si-rich multifunctional DLC coating deposited on 1020 steel and tested against 52100 steel pins was analysed. Unlubricated reciprocating pin-on-disk tests were performed using a high pressure tribometer (HPT) under different atmospheres (air, CO_2 and R600a). The tribological behaviour (friction coefficient and wear rate results) was analyzed using laser interferometry, scanning electron microscopy and micro Raman spectroscopy. Samples tested in R600a environment presented the lowest friction coefficient and the lowest wear rate for both body and counter-body. The evolution of the friction coefficient during the test duration time presented a significant transient with later stabilization around a constant value. For tests conducted in R600a, an initial period after which the friction coefficient increased up to a maximum was observed. On the contrary, in the presence of CO2, after a quick decrease, the friction coefficient changed gradually and reached a relatively steady value. In air, after a quick initial decrease, the friction coefficient started to increase gradually to a steady-state value. The wear rate of samples tested in R600a atmosphere presented the lowest wear rate. The wear rate increased when tests were performed in CO2 and air (33% and 52%, respectively). The wear rate of the counter bodies increased significantly when tests were performed in CO2 and air (175% and 266%, respectively). There are no remarkable differences between the EDS and Raman spectra of the wear scar presented in the disks. The strong presence of the graphitic G-band in the spectra of tribolayers produced in R600a atmosphere is likely to induce their superior tribological performance.

Seung Min Yeo et al., [6] Due to favourable tribological performance, PTFE- and PEEK-based polymeric coatings have received interest in air-conditioning and refrigeration compressor applications, as a potential solution to supplement and potentially replace conventional oil lubricants. The literature in this area is somewhat scarce, especially on the tribological performance of PTFE- and PEEK-based polymeric coatings under aggressive conditions simulating compressor operation. In this work,

several PTFE-, PEEK-, resin- and fluorocarbon-based polymeric coatings, coated on grey cast iron were tribologically evaluated using a specialized tribometer under compressor specific conditions, that included oscillatory motion (simulating piston-type compressors) and unidirectional motion (simulating swash plate compressor operation). The coatings showed good to excellent tribological performance, and in general PTFE-based coatings exhibited better friction and wear behaviour than the rest of the coatings, including PEEK-based coatings. Long-term durability experiments also showed the superiority and suitability of PTFE/Pyrrolidone coating for potential use in oil-less compressors (where oil-less conditions refer to operation in the absence of any liquid lubricant).) Higher friction coefficient values in the range of 0.1–0.2 and wear rate values of 105 mm3 /N m were measured under oscillatory conditions. Better performance with lower friction coefficient values of 0.04–0.1 and wear rates of 107 mm3 /N m were measured under unidirectional conditions. Under both operating conditions (but more so for unidirectional), polymeric coatings exhibited acceptable to superior tribological performance, under aggressive oil-less compressor conditions, and thus are likely viable candidates for the next generation of oil-less compressors. PTFE-based coatings (PTFE/Pyrrolidone and PTFE/MoS2) generally performed better than PEEK-based coatings (PEEK/PTFE and PEEK/Ceramic) under both piston-type (oscillatory motion) and swash plate (unidirectional motion) compressor conditions, which was not the case for bulk polymer blends (where typically PEEK composites filled with PTFE performed best). The effect of polymer coating wear debris, serving as a solid lubricant on the hard substrate surface, was shown to be more dominant in determining the overall wear behaviour of polymeric coatings than the mechanical properties of the polymer coating itself. The structural changes in the PTFE coatings from semi-crystalline to amorphous caused by the coating process, resulted in very fine wear debris enhancing its lubricity. PEEK-based polymer coatings were still exhibiting crystalline structure after the coating process, due to its high crystallizing speed, thus resulting in large and flake-like wear debris. Durability or time-to-failure (3-h duration) unidirectional testing corresponding to 40.5 km sliding distance showed superb friction and wear behaviour of PTFE-based coatings, especially PTFE/Pyrrolidone-2, thus demonstrating its potential applicability for use in oil-less compressors.

B. Raja et al., [7] In a refrigerant compressor, improvement in performance such as reduction of various electrical and mechanical losses, reduction of gas leakage, better lubrication, reduction of suction gas heating etc. can be achieved by maintaining a low temperature rise inside the compressor. Proper selection and location of an internal over load protector relay, estimation of heat transfer coefficient and winding insulation coefficient are also vital in enhancing the performance. In this context it is necessary to understand the temperature distribution inside a compressor for an optimal design. In this paper, a numerical model has been created and a heat transfer analysis for a hermetically sealed reciprocating refrigerant compressor is presented. The temperature distribution inside the compressor has been obtained taking into consideration the various heat sources and sinks and compared with experimental results. The maximum temperature was observed at the rotor which was 427.5 K. The deviation of the predicted rotor temperature from that of experimental value is 5.5% only. A good agreement was found between experimental results and that predicted in the numerical analysis. In the design process of a hermetically sealed compressor, the over load protection relay (OLP relay) selection and positioning plays an important role. It has to be selected and located by considering the factors such as occurrence of maximum operating temperature in the full flow domain in the compressor, the thermal stability of the protective coatings and binders applied over the motor coil, the thermal stress inside the laminated core of the motor coil and the stability of the lubricating oil. As the temperature at various points inside a compressor at various operating conditions could be obtained without tedious and expensive experimental works, this model could be used to predict the temperature distribution/occurrence of maximum temperature in the compressor flow sections to fix the OLP position. The validity of the model was confirmed based on the comparison of predicted and experimental temperature levels as given in Table 1. Further the model enables the designer to predict the actual entry temperature of refrigerant into the compression chamber after picking up heat from the rotor and stator windings in the shell. This is quite useful in estimating the actual volumetric efficiency of the compressor during operation that is quite beneficial in system simulation studies.

Miguel B. Demay et al., [8] Compressor speed is a very important parameter when testing hermetic compressors. Its measurement is routine in the refrigerator compressor industry, either to evaluate parameters such as capacity, power consumption, and

coefficient of performance (COP), or as an indicator of steady-state operation. However, there are some difficulties associated with measuring the speed of hermetic compressors, mainly concerning uncertainty and time constraints. This study presents some hermetic compressor speed measurement techniques, based on quantities that can be measured outside a compressor shell. In this study it was possible to measure compressor speeds through these techniques with an uncertainty of less than 1 rpm in a measurement time of 5 s. This paper presented some techniques for measuring the speed of hermetic compressors through quantities which can be measured externally, for instance, the supply current and discharge pressure signals. Some mathematical techniques that provide speed measurements through the use of these signals were also applied. Two techniques, FFTInt and CZT, were shown to provide excellent results. With an acquisition time of only 5 s it was possible to reach a maximum error smaller than 0.31 rpm, with a confidence level of 95%. These methods have been applied to measure compressor speed in performance tests at Whirlpool, at the EMBRACO plant (Joinville, SC, Brazil), which plans to apply them in other plants. The measurements have been successfully performed on many different compressor models within a wide capacity range, and even on variable-capacity compressors, indicating the applicability of the method to a wide variety of hermetic compressor types and sizes.

Sun Zhe et al., [9] As an important parameter of hermetic compressor, the speed value has direct effects on the cooling capacity, control performance and power consumption of the refrigeration system. Therefore, modern refrigeration industry has put forward higher requirement for measuring the speed of the compressor. Conventional speed measurement methods are based on shell vibration and discharge pressure fluctuation. However, shell vibration-based methods require more elaborate instrumentation, leading to more complex and expensive procedure, as well as unsatisfied accuracy. Discharge pressure fluctuation-based methods can destruct mechanical structure and influence the state of fluid flow. This paper proposed a measurement method based on slip signal and presented a Hilbert transform-based algorithm to improve the extraction accuracy and real-time measurement, and to reduce the complexity of the measurement system. Compared with the standard measurements generated by the compressor with encode, under the 1 s sampling time, it is possible to reach a maximum error smaller than ± 1 rpm, which can prove broad application prospect in the refrigeration industry. This paper

proposed a current-based speed measurement method for fully enclosed refrigeration compressors. The method has the advantages of fast measurement speed, high measurement precision, simple system construction, break throughing the bottlenecks in measuring the speed of fully enclosed refrigeration compressors. The method was verified on the standard fully enclosed refrigeration system test platform. The sampling frequency was 1 kHz and the sampling time was from 2 s to 0.5 s. Based on the experimental comparison of the three main measurement methods existing, this current-based method seemed to be most advantageous than that of shell vibration and pressure pulsation, which can provide a broad application prospect.

J. Rigola et al., [10] The aim of this paper is the detailed analysis of different well-known thermodynamic efficiencies usually used to characterize hermetic compressors. Attention is focussed on the volumetric efficiency, the isentropic efficiency, and the combined into their main components (physical sub-processes) to get deeper insight on the overall behaviour. The volumetric efficiency is split into partial efficiencies related to pressure drop and heat transfer effects, supercharging effects, super discharging effects, leakages, etc. The isentropic efficiency is detached using two different points of view: the work associated to the individual sub-processes (compression, discharge, expansion, suction), and the work associated to the under pressures, overpressures, and between the inlet and outlet mean compressor pressures. Finally, the combined mechanical– electrical efficiency is related to the heat transfer losses/gains, and to the exergy transfers and exergy destroyed. Even though some of the concepts introduced in the paper can be applied to different kinds of compressors, the discussion is specially focussed on hermetic reciprocating compressors. An advanced simulation model developed by the authors has been used to generate data to illustrate the possibilities of the detailed thermodynamic characterization proposed. The criteria developed are useful tools for comparison purposes, to characterize compressors, and to assist designers during the optimization process. A detailed analysis of some well-known thermodynamic efficiencies usually used to characterize compressors has been presented with special emphasis on hermetic reciprocating compressors used in the refrigeration field. Attention has been focussed on the volumetric efficiency, the isentropic efficiency, and the combined mechanical–electrical efficiency. A procedure is presented to detach these efficiencies into their main components (physical sub processes). The volumetric

efficiency is split into different efficiencies related to pressure drop and heat transfer effects, supercharging effects, super discharging (or reverse flow) effects, leakages, etc. The isentropic efficiency is detached using two different points of view: the work associated to the individual sub-processes (compression, discharge, expansion, suction), and the work associated to the under pressures, overpressures, and between inlet and outlet mean compressor pressures. The combined mechanical– electrical efficiency is related to the heat transfer losses/ gains, and also to the exergy transfers and exergy destroyed. Some illustrative examples are presented to show the possibilities of the thermodynamic performance characterization proposed. The results have been generated by a certificated and validated advanced simulation model of the thermal and fluid dynamic behaviour of hermetically sealed reciprocating compressors. The results show the influence of different design and operating parameters, such as the compression ratio, mean compressor inlet temperature, ambient temperature, cylinder–piston gap, clearance volume, valves thickness. The criteria developed are useful tools for comparison purposes, to characterize compressors, and to assist designers during the optimization process.

N.P. Garland et al., [11] This paper describes the environmental impacts of hydrocarbon refrigerants deployed in the domestic refrigerator hermetic compressor. In-use durability is examined from a tribological viewpoint. Experimental tribological information is presented from physical test procedures involving sliding tests to establish wear mechanisms and friction coefficients within critical components. Hydrocarbon refrigerant R600a is compared with hydroflourocarbon R134a using aluminium on steel samples within a novel pressurised micro-friction test rig. The refrigerant R600a is tested for its influence upon the tribological performance of mineral oil (MO) and poly-ol-ester (POE) lubricant, whilst an R134a/POE charge combination is used as a benchmark. Tribological data is used to model long-term performance and subsequent environmental costs. The performance of refrigerant/lubricant charge combinations are evaluated within the pressurised refrigerant environment. The best performing charge combinations, for wear, were those that established and sustained a boundary film upon the counter-face of the pin sample. The additive MO samples had a good boundary film on the pin and almost no wear at all on the plate, for these samples wear rates were low. In the case of the additised POE lubricant and refrigerant combinations deposition was present at the plate

but not at the pin sample, under these conditions initial wear rates were high but reduced as the contact geometry became more favourable. The lubricant with the lowest wear rate at the pin counter-face was the non-additised MO. The higher contact stress and reduced gudgeon pin bearing area of the R134a compared with the R600a compressor leads to reduced performance over time, despite the lower wear rate achieved for the R134a POE charge. The R600a compressor continues to perform at the end of its 15-year cycle where as the performance of the R134a compressor deteriorates rapidly at, and beyond, 15 years. This fall off in performance results in a greater environmental burden compared to the R600a.

Sathuramalingam Pillay Darminesh et al., [12] Naturally, biodegradable oil has better viscosity index, pour point, flash point, good tribology properties and its environmental friendly. Even though biodegradable lubricant is one of the best choice for lubrication purposes, however the properties are slightly lesser than mineral oil. A common solution for this problem is to provide effective additives into the base stock of biodegradable oil which leads to significant improvement to the lubricant by enhancing thermal properties, tribological properties and anti-oxidation capability. Nanoparticles are a type of effective additives which provides promising approach to enhance the biodegradable lubricant's properties. In this article, we reviewed the current progress and recently published data related to biodegradable lubricant, nanoparticles and its improvement on the biodegradable lubricant properties. Nature form of vegetable oil has good physical properties to become lubricant due to its triacylglycerol structure with long fatty acid chains and presence of polar groups which makes the oil with amphiphilic character but its main restriction is poor thermo-oxidation property. However, the natural form vegetable oil can be improved by techniques such as trans esterification, epoxidation, hydrogenation and post-esterification. These techniques will eliminate the β carbon in ester chain and enhanced the lubricity, viscosity, thermal and oxidative stability. Additive can been used to enhance the properties of lubricants extracted from vegetable oil. However, most of additives are not compatible for the vegetable oil and some additive are not advisable due to high impact on environment and endanger human health. Nanoparticles are one the suitable additive for the vegetable base oil. Though, the size, shape, and concentration amount has great impact on the tribological properties of nanolubricant. Based on the reviews above, the optimum size of nano-additive in range

of 20–70 nm whereas the shape in quasi-spherical and optimum concentration in range of 0.2–1 wt%. The CuO, Ti02 and Si02 are common metal oxide nanoparticles which exhibits good enhancement as nano-additive. The CuO has been stated that it carriers good tribological properties with self repairing characteristic, whereas the SiO2 has good dispersion homogeneity and stability over long period. The modified surface of nanoparticles with chemical also can further improve the characteristics compared to unmodified nanoparticles. Other than that, the hybrid nanoparticles exhibit better performance than single additive nanoparticles.

C. Ciantar et al., [13] Hydrofluorocarbons are alternative refrigerants receiving attention for use in domestic refrigerating systems. New synthetic lubricants are required with these working fluids to ensure lubricant suitability. The objective of this experimental investigation is to compare the tribological performance of the newly developed polyvinylether PVE synthetic lubricant to its polyol ester POE counter-part. Experimental setups were varied using actual hermetically sealed refrigerating compressors. This investigation included an evaluation of the conforming contact between the small end of the connecting rod and the gudgeon pin. This was done in conjunction with observations of the large end of the connecting rod as well as the compressor valve plates. Observations were carried out using light microscopy, scanning electron microscopy SEM, energy dispersive X-ray EDX micro-analysis and X-ray photoelectron spectroscopy XPS analysis. The wear mechanisms typical of the removal of material between sliding surfaces have been observed to occur for both of the two lubricants tested. No clear-cut distinction between the lubricating performance of either of the two lubricants could be made. The considerable improvements in lubricating performance for the newly developed PVE have not been exhibited. The PVE seemed to be more chemically active on the interfacing surfaces, in particular with that of the aluminium. This led to the general observation that wear on the steel pin was more significant for the POE type although the aluminium connecting rod seemed to be more susceptible to the PVE type. The surface reactions observed to occur on the aluminium samples, in particular for the PVE due to their state of degradation, call for further investigation. The mechanisms involved were complex and a feasible explanation has yet to be found. Compounds observed using the XPS technique showed that the protecting film deposit on the valve plate was less pronounced for the PVE lubricant as compared

to its POE counterpart. Under the experimental parameters experienced here, no carboxylic compounds were observed for either of the synthetic lubricants tested.

2.2 Motivation

Cooling appliances now a days become very important due to their multiple applications in the field of human comfort and preservation of food items. Compressor is the heart of every cooling device. Hermetically sealed reciprocating compressor is widely used in AC's and domestic refrigerators which forms a very large part of cooling industry. Thus research should be carried out on life expectancy of hermetically sealed compressor. So, in this project research is done on wear and tear of reciprocating compressor and how to minimize it.

2.3 Research Gap

- A very few research have been done on material modification of linear reciprocating compressor.

- No new alloy have been casted or tested as the material for piston in hermetically sealed compressor.

- Coatings are generally done to reduce the wear in reciprocating parts, but not implemented till now.

CHAPTER 3: TOOL USED

3.1 Tribometer

A tribometer is an equipment that is used for measuring the wear between the two surfaces which are in contact with each other. Tribometer also measures the coefficient of friction and frictional forces according to the conditions of 1load, frequency and temperature given by the user. A tribotester is the name given to the machine that analyses the calculation of wear. It was invented by a Dutch scientist in 18th century.

The principle of tribometer can be explain by the simple experiment in which a block is at rest at table called sitting mass while a mass is hanging from the cable. For determining the co-efficient of friction, the condition of just sliding is taken into consideration, the weight of hanging mass is increased until the sitting mass starts moving.
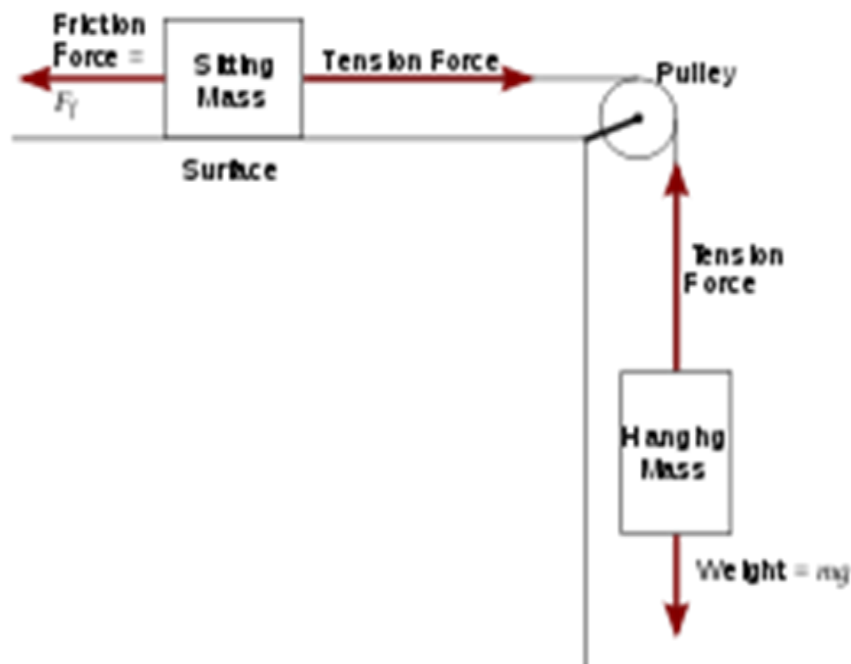
Fig.3.1: Principle of tribometer [source: R. Binder et al.,]

$$F=\mu N \qquad\qquad (3.1)$$

Where N, the normal force, is equal to the mass (mass x gravity) of the sitting mass (m_T) and F, the load force, equal to the weight (mass x gravity) of the suspended mass (m_H). To determine the motor friction coefficient, the suspended mass increases or decreases until the mass system moves at constant speed. In both cases, friction coefficient is simplified to the ratio of two blocks:

$$\mu = m_H/m_T \qquad\qquad (3.2)$$

In linear reciprocating tribometer the calculation of wear is done directly by measuring the weight of specimen after test duration. The calculated Weight is then subtracted from the initial weight of specimen to find out the wear directly. Further investigation for wear patterns can be done with help of optical microscope, scanning electron microscopy etc.

3.1.1 Ducom Linear Reciprocating Tribometer

The Ducom Linear Reciprocating Tribometer is designed to allow users to characterize the tribal offers of materials and lubricants in a wide range of operating conditions, ranging from low corrosion conditions to large linear slip conditions. If it can be used effectively to study bulk materials, coatings, lubricants and additives. The Linear Reciprocating Tribometer can accommodate a variety of geometric shapes to create contact points, lines, and regions. This system is controlled by the computer and includes a data acquisition program that can be used to obtain, view, and report results.
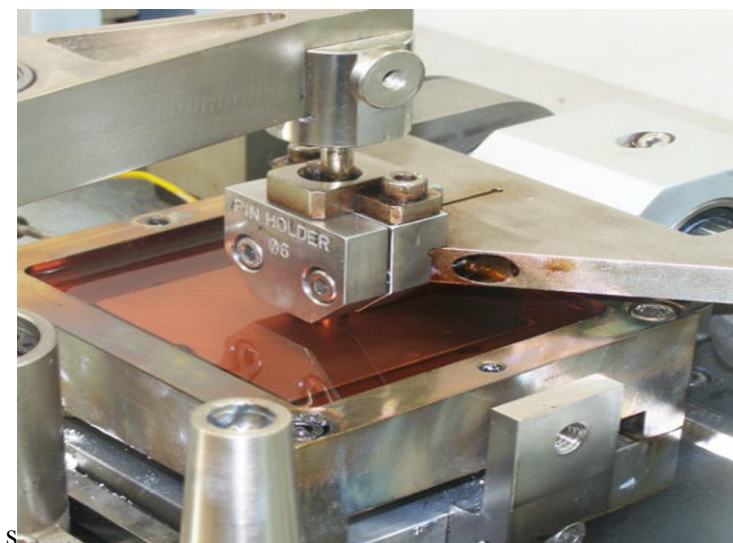
Fig. 3.2: Linear reciprocating tribometer [source: DTU]

Technical specification

Table 3.1: Technical specification of tribometer

Parameter	Fretting Wear Tester (FWT)	Linear Reciprocating Tribometer (LRT)
Load Range	Up to 200 N	Up to 200 N
Frequency	1 to 200 Hz	4 to 40 Hz
Stroke Range	100 µm to 300 µm	1 mm to 30 mm
Compound Wear Measurement	0 to 1200 µm	0 to 1200 µm

3.2 Optical Microscope

A conventional microscope is a simple type of light microscope which uses a beam of light and a few lens to generate image. These type of microscopes are very common and generally uses in homes, school and small laboratory set ups. These microscopes uses an ordinary set of camera for capturing the images, the images are then recorded and analysed. With advancement now a days CMOS and CCD cameras are used which allow digital image to be captured these types of camera directly capture the images without the use of lens and these images can directly be analysed. Alternatives to optical microscopy that do not use visible light include microscopic scanning of electron microscopes, microscopic electron microscopes, and microscopic transport vectors.

Fig. 3.3: Optical microscope [source: DTU]

3.3 Scanning Electron Microscope

Scanning electron microscopy is the latest technology that uses a beam of electron to fall upon the sample, when the beam fall upon the specimen it produces different signals when interact with different components in samples. Raster pattern is used to analysed the beam, the detected signal is mixed with beam position to generate an image. The electrons at various depths interact with the atoms to produce different signals, these signals are further analysed to produce an image. The other types of signals that are being formed are secondary electrons (SE), reflected or back scattered electrons (BSE), characteristics X-ray and light (CL), absorbed current and transmitted electrons.

3.3.1 Principle and capacity

Secondary electrons are emitted form a close distance, thus SE produce a high quality image of the specimen, whereas in case of BSE the electrons are emitted from a distance so the quality of image in case of BSE is comparatively very low as compared to SE images. But these have good linkage of signal with the atomic number thus BSE is used for analytical SEM with spectra of X-ray characteristics. BSE can provide information about the distribution of elements in the specimen but it does not provide the information about the identity of the element. BSE used with X-ray replaces the electron in the specimen, the intensity or the energy of these filling electrons can be measured with the help of X-ray spectroscopy.

3.3.2 Sample Preparation

Sample must be of specific standards to be fitted inside the SEM. The samples are first holded in the sample holder where necessary adjust are done according to the height of specimen and an adhesive tape is applied to increase the conductivity of the specimen. A specimen must be properly mounted to withstand the high vaccum conditions and high energy beam of electrons.

Coating of low atomic numbers material with the high atomic numbers can increase the signal/noise ratio which results in getting better images of objects. The coatings of

material such gold, osmium, graphite, palladium, tungsten, iridium, platinum are done to increase the conductivity.

Fig. 3.4: Scanning electron microscope [source: IIT, delhi]

3.4 Hardness Tester

Hardness is the measure of local deformation caused by mechanical forces or due to corrosion by environmental conditions. Hardness of material depends upon the arrangement of molecules in them, the hardness of certain material are high whereas hardness of some material are quite low. The hardness of the material is depended on the binding of particles within them, but the behaviour of particles under forces changes thus there are many methods to measure the hardness of the solid like hardness of recoil, hardness if indentation, hardness of scratching.

3.4.1 Indentation Hardness

The indentation hardness measures the resistance of a sample to distort materials because of the constant loading pressure of the sharp object. Hardness tests are used primarily for indentation in the fields of engineering and metals. The tests work on the basic premise for measuring the critical dimensions of the indentation left by the center of distance with the specified dimensions and loads. Common indent measurements are Rockwell, Vickers, Shore, Brinell, and others.

Fig. 3.5: Hardness tester [source: CAPEIR, DTU]

CHAPTER 4: RESEARCH METHODOLOGY

Tribological performance of modified piston-cylinder assembly of hermetically sealed compressor is carried out using linear reciprocating compressor. To carry out the research a rod of Aluminium doped with Copper, Nickel and Magnesium is casted using sand casting process. This rod represents the piston of compressor while the cylinder is represented by cast iron plate which was machined from cast iron block using power hacksaw.

Casting of rod is done in foundry using simple pouring of molten Aluminium with nickel, copper and magnesium in sand mould and allowed it to cool to room temperature. The rod is then further machined for surface finishing using emery paper of different grits. The cast iron plate is machined down from a cast iron block using power hacksaw and trimmed using bench grinder for precise dimension and then surface finished using emery papers of different grits.

Testing of samples is done using Linear Reciprocating Tribometer, specimens are rubbed against each other according to user provided conditions and then results of frictional forces, coefficient of friction and wear is noted down. Aluminium rod is rubbed against plate made of cast iron under the same conditions as that there are in hermetically sealed compressor. The COF, FF is recorded and the wear is calculated by measuring the loss in weight of specimen. Specimens are weighted before the experiment and they are again weighted after the experiment to calculate the loss in weight and subsequently wear.

The casted sample is further tested for optical microscopy, Scanning Electron Microscopy and Hardness testing. For optical microscopy the sample is hard mounted using Bakelite and then surfaced finished using emery paper and then polished using Alumina paste. The polishing is done to remove all the scratches from the surface. Further etching is done to reveal the structure of the alloy, etching is done using dil. sulphuric acid and dil. Nitric acid to reveal the crystal structure of material. The

Microscopic images sample is taken using one thousand magnification. The images reveal the crystal structure of copper, nickel and aluminium.

Scanning Electron Microscopy with EDAX is done to study the crystal structure of sample as well as to study the composition of sample. The samples is prepared by polishing it against emery paper and then then polished with alumina paste no further requirement of etching is needed. Energy dispersive X-ray spectroscopy is done to study the composition of sample and to determine the constituents of the sample.

Hardness testing is done to measure the hardness of the sample. The sample is Bakelite mounted and then indentation is done to sample to study the hardness of the sample.

Design of experiments (DOE) is an optimization technique that works on cause and effect relationship and it is used in this experiment to optimize the value of wear using different conditions of temperature, load and time. Different sets of reading are evaluated using DOE approach and they are tested in software to get the optimized result.

Nine sets of readings (L_9 approach) have been taken and they are further tested to get the value of wear. This value of wear is further tested using MINITAB software to get the optimized value of wear under the given sets of condition.

CHAPTER 5: RESULTS AND DISCUSSIONS

In linear reciprocating tribometer the calculation of wear is done directly by measuring the weight of specimen after test duration. The calculated Weight is then subtracted from the initial weight of specimen to find out the wear directly. The load is applied vertically down through the sample pin against the flat sample horizontally. Normal load, stroke length, frequency and type of oscillations, test temperature, lubricant, and test duration and air environment are selected from one of the two procedures.

The test method involves a reciprocal skid where changes in the speed of slippage and direction of motion occur during the test, constant velocity conditions are not maintained. The method by which the speed is varied over time is determined by the automatic design that drives the disc sample or disc back and forth.

5.1 Sliding distance

To compute the siding distance in metres or number of cycles, use the following:

$$X = 0.002 \times t \times f \times L,$$

$$N = t \times f;$$

Where,

X = total sliding distance of pin,

N= number of cycles in test;

t= test time, secs,

f= oscillating frequency in Hz and;

L=length of strokes mm.

The value of sliding distance remain same for all the sets of value because only value of load have been changed during the experiment which does not have any effect on value of sliding distance. The value came out to be 120m.

5.2 Wear rate

Wear rate is defined as wear (change in weight of specimen) to the sliding distance. Wear rate of pin and plate have been calculated using sliding distance and plotted in these tables:

Table 4.1: Wear in Pin

S.No.	Wear in pin	Calculated wear rate
1	0.0011gm	0.000009166
2	0.0001gm	0.00000083
3	0.0005gm	0.00000416
4	0.0001gm	0.0000083

Table 4.2: Wear in Plate

S.No.	Wear in plate	Calculated wear rate
1	0.0022	0.0000183
2	0.0044	0.0000366
3	0.0030	0.000025
4	0.0024	0.00002

The average value of wear in pin and plate are 0.00000748 gm/m and 0.0000249gm/m.

Case 1: When the applied load is 5N, frequency is 50Hz and experiment run for 10 minutes. The graph between co-efficient of friction and time is shown below in fig. 5.1.
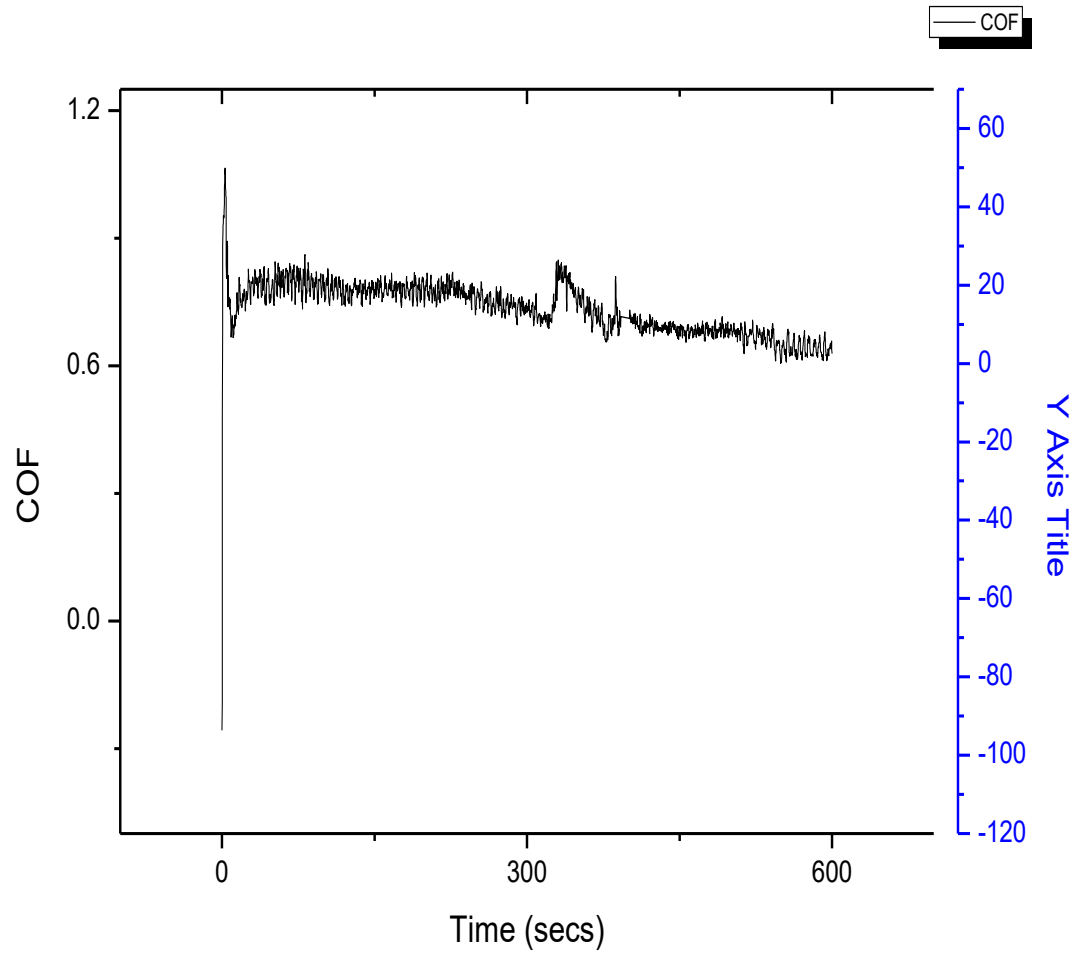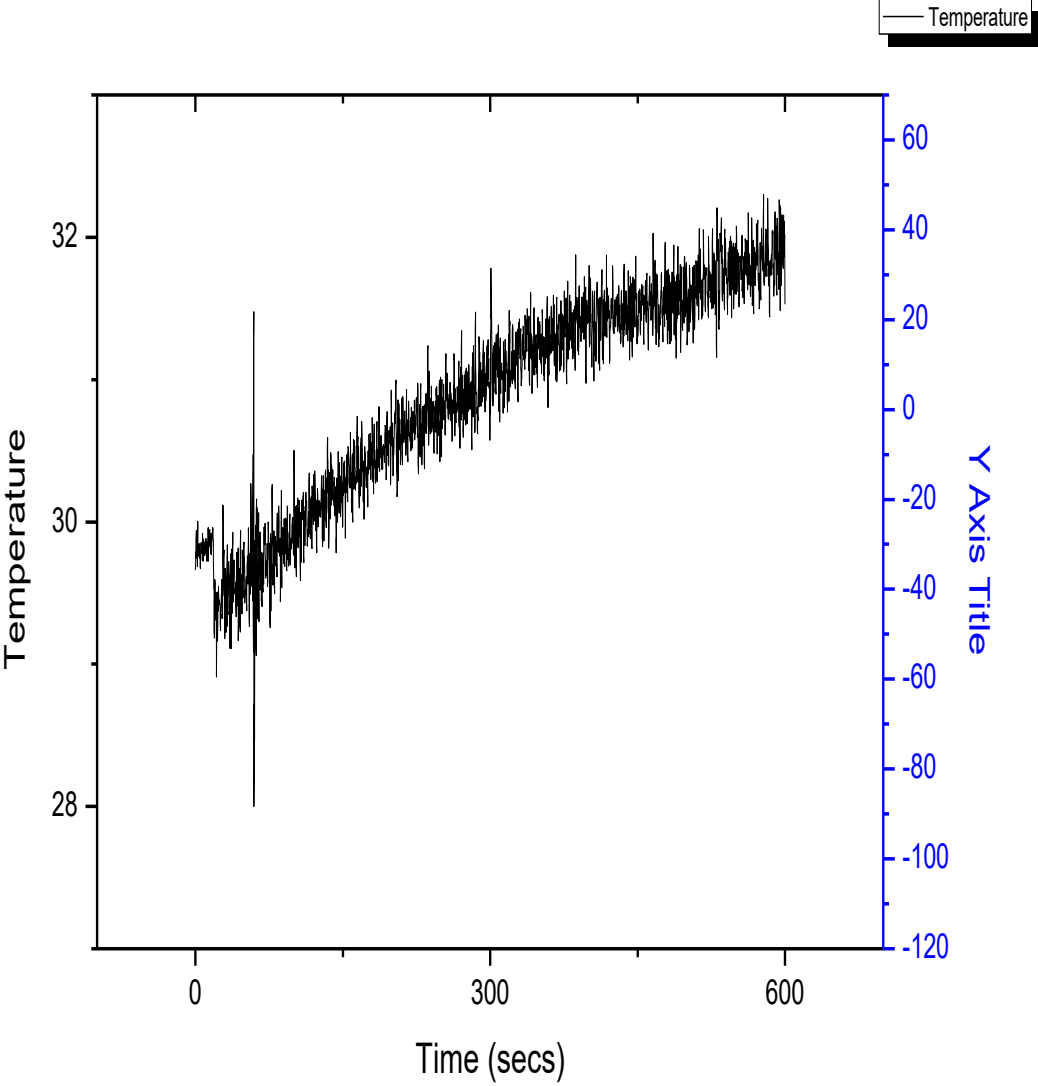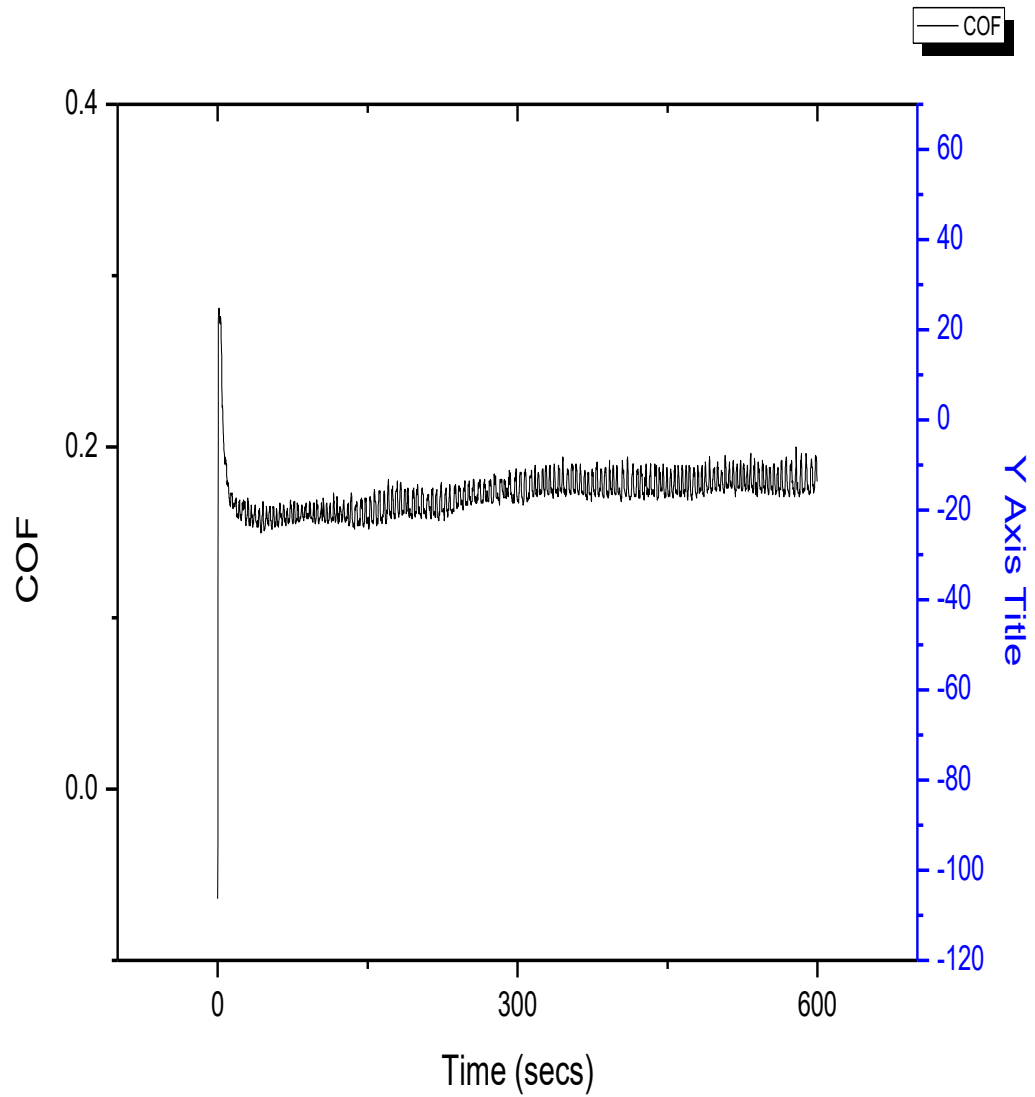

Fig. 5.1: Graph of COF versus Time

Case 2: When the applied load is 5N, frequency is 50Hz and experiment run for 10 minutes. The graph between frictional force and time is shown below in fig. 5.2.
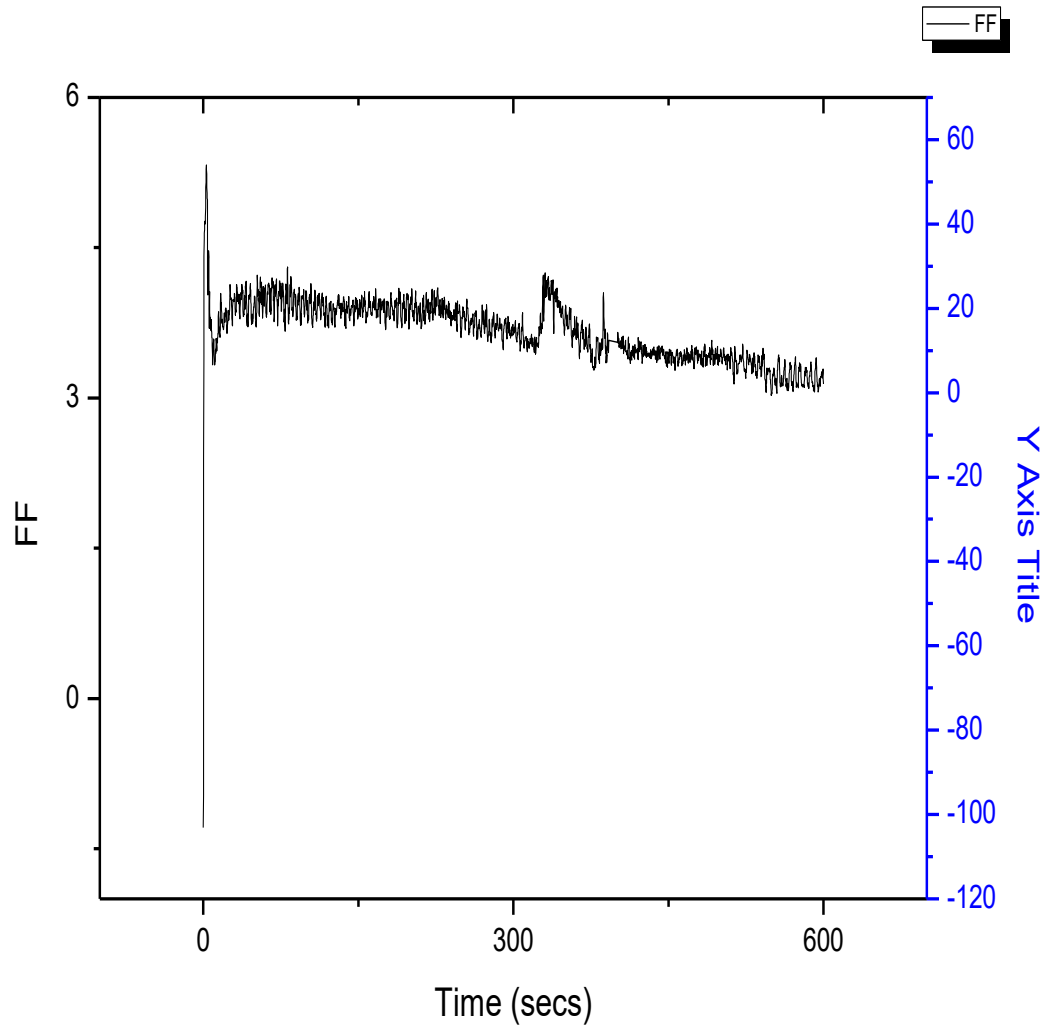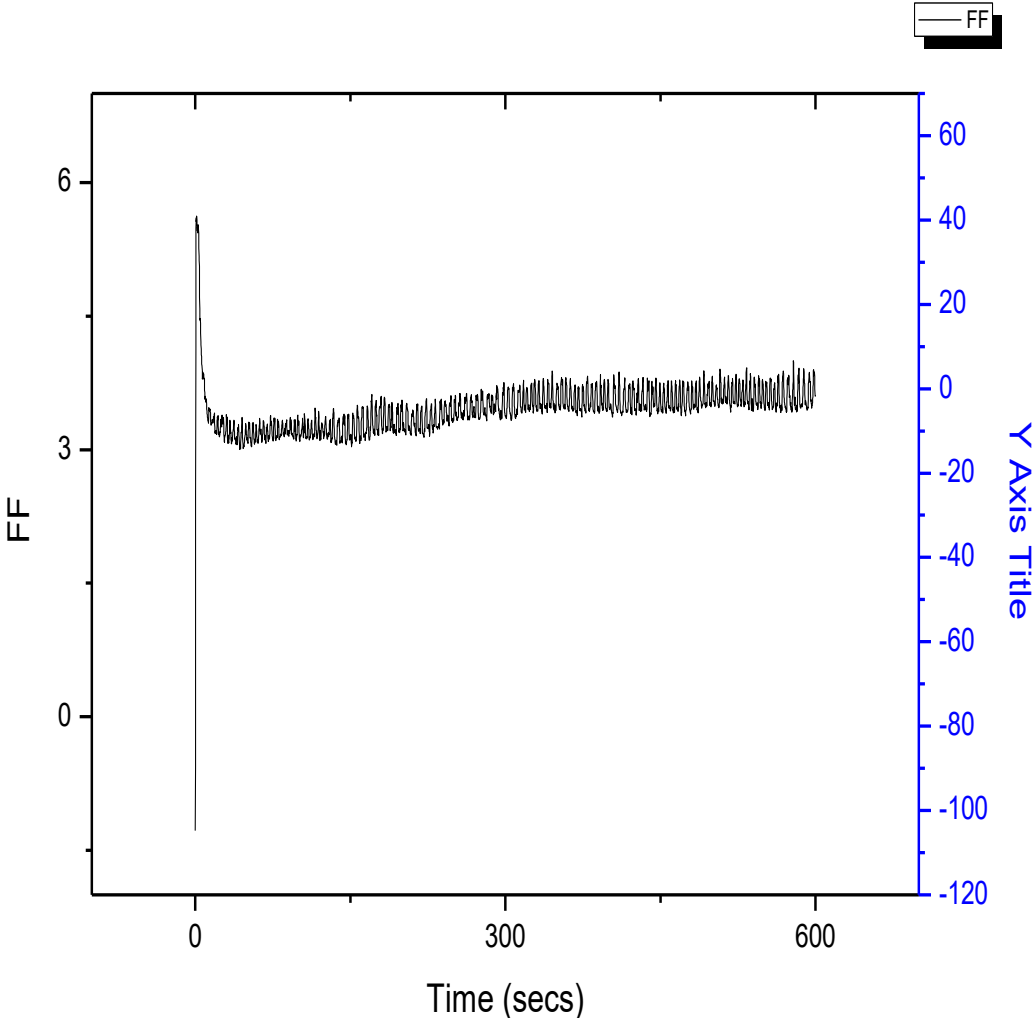

Fig. 5.2: Graph of FF versus Time

Case 3: When the applied load is 5N, frequency is 50Hz and experiment run for 10 minutes. The graph between temperature and time is shown below in fig. 5.3.
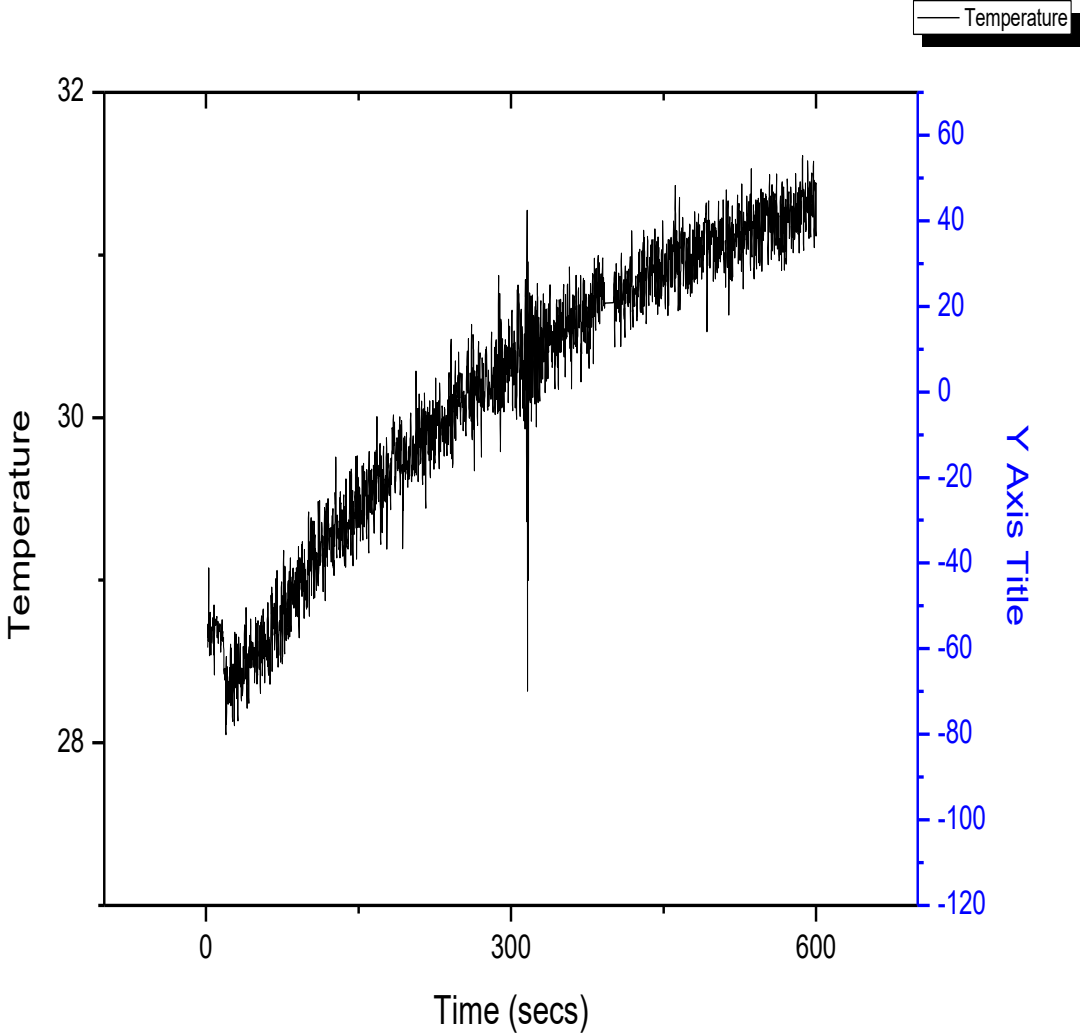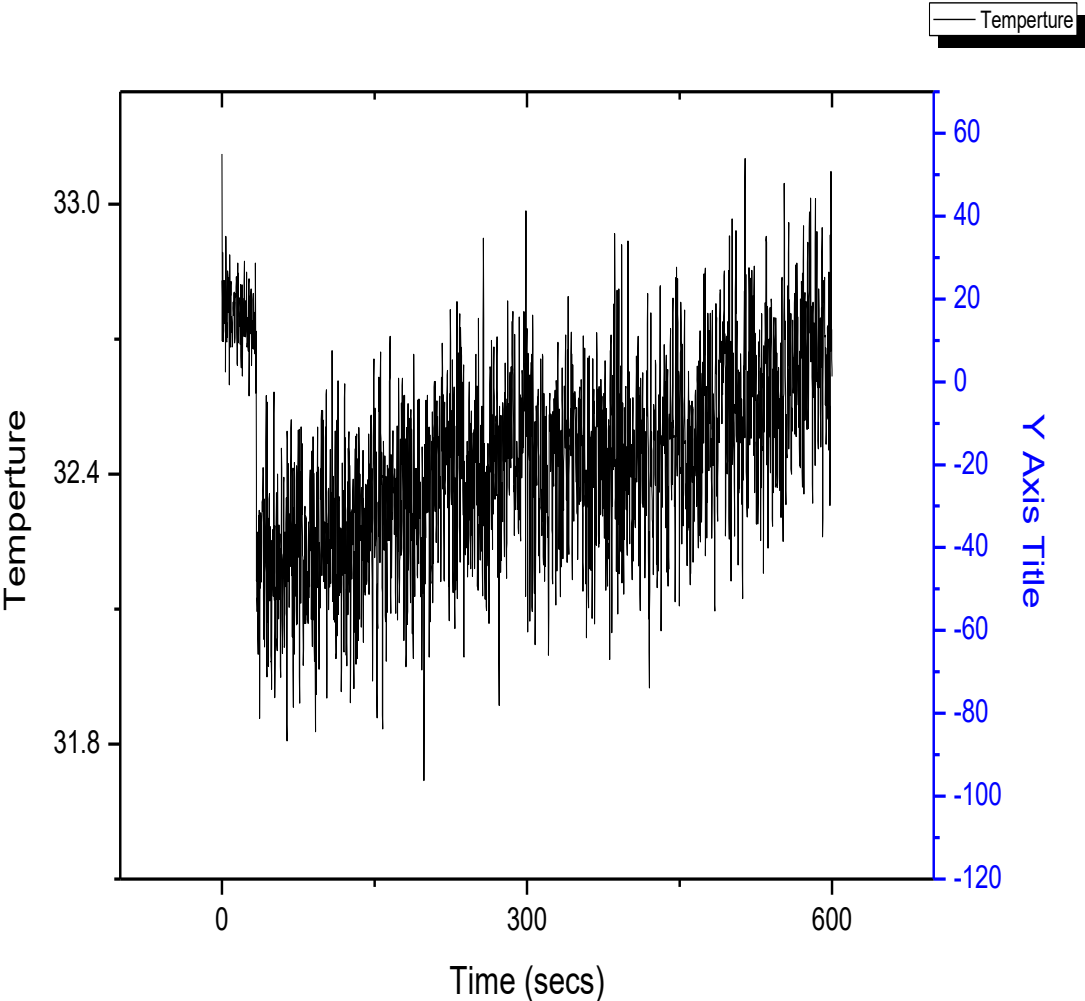

Fig. 5.3: Graph of Temperature versus Times

Case 4: When the applied load is 15N, frequency is 50Hz and experiment run for 10 minutes. The graph between co-efficient of friction and time is shown below in fig. 5.4.
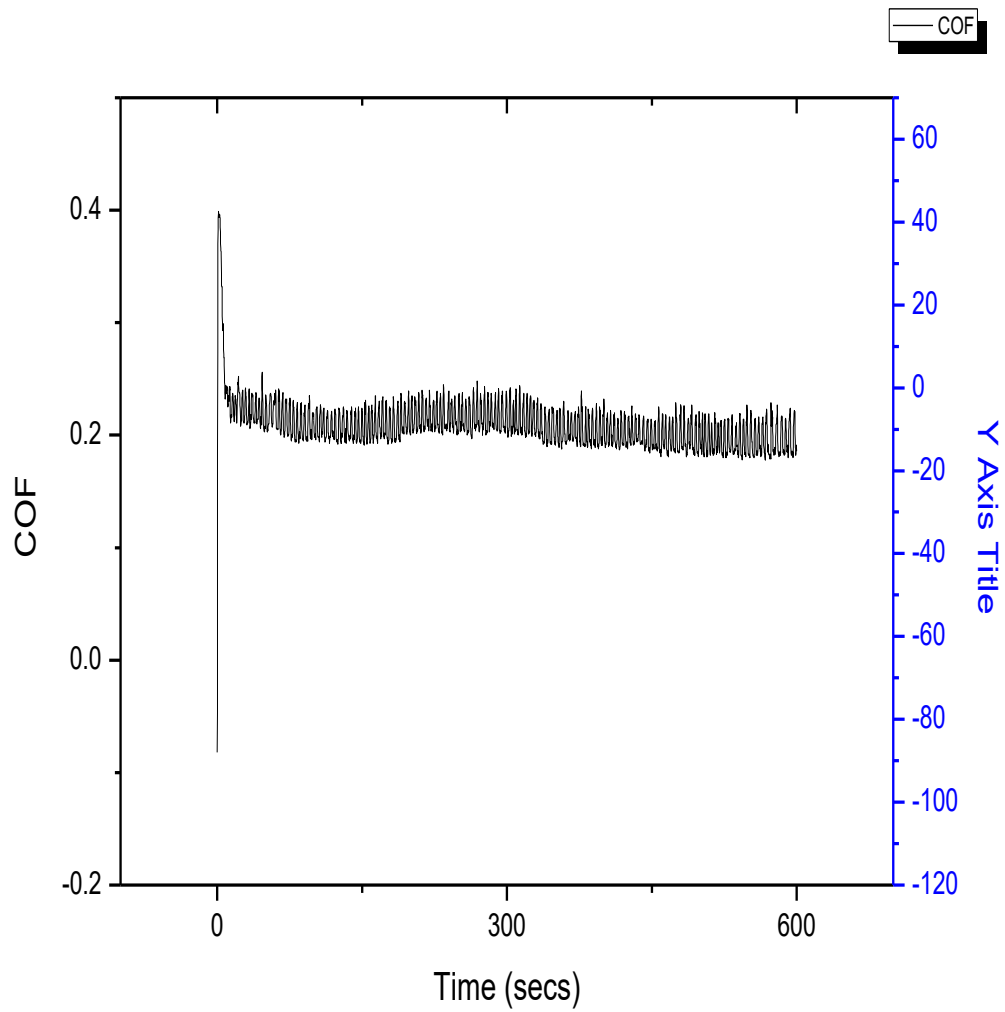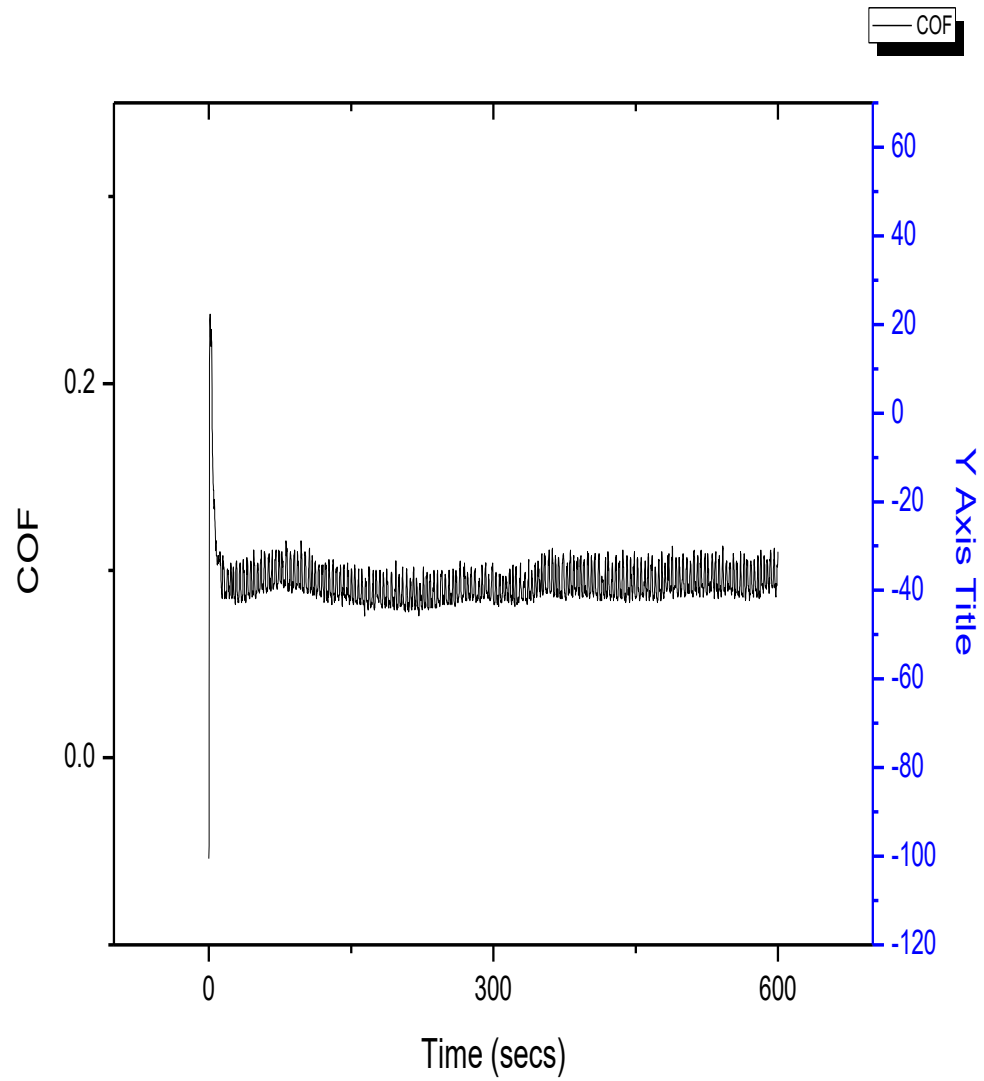

Fig. 5.4: Graph of COF versus time

Case 5: When the applied load is 15N, frequency is 50Hz and experiment run for 10 minutes. The graph between frictional force and time is shown below in fig. 5.5.
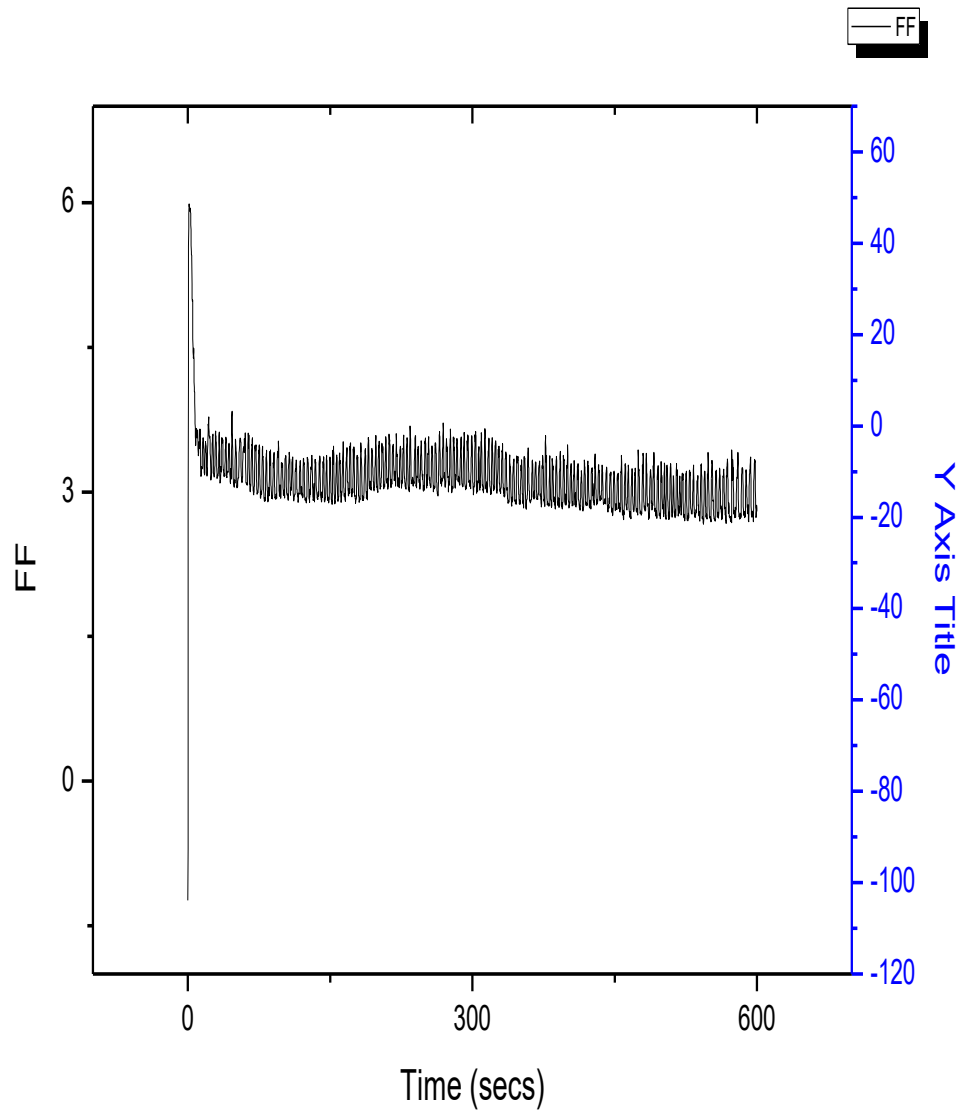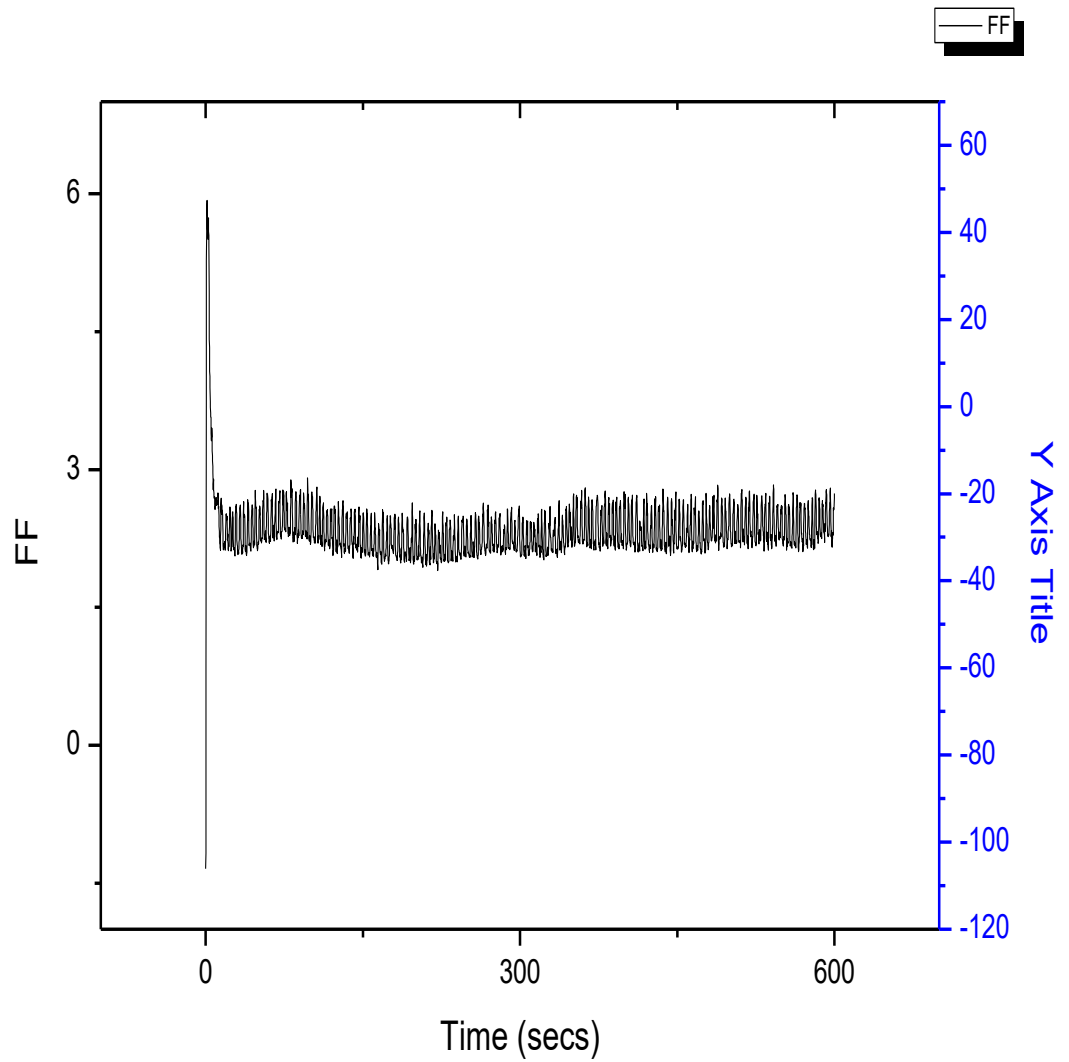

Fig. 5.5: Graph of FF versus Time

Case 6: When the applied load is 15N, frequency is 50Hz and experiment run for 10 minutes. The graph between temperature and time is shown below in fig. 5.6.
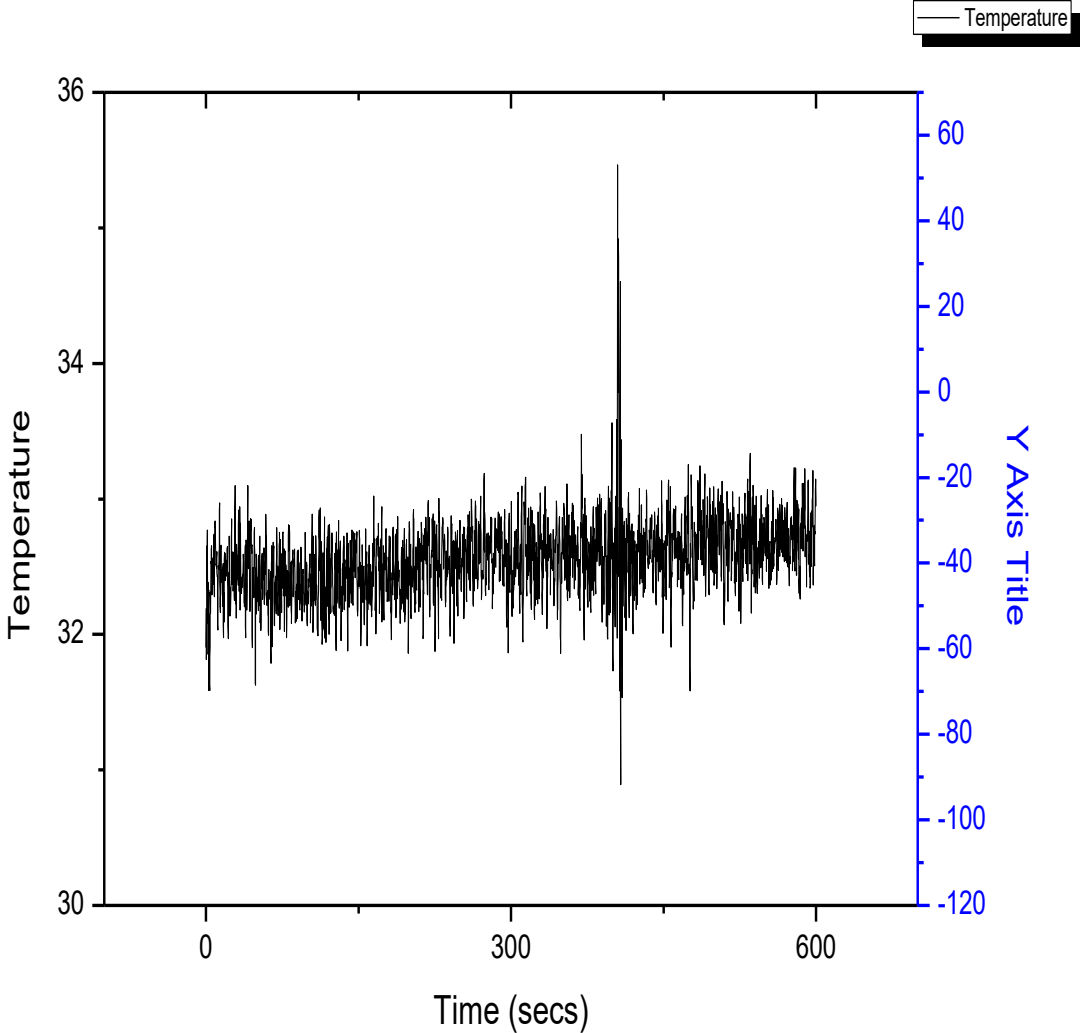

Fig. 5.6: Graph of Temperature versus Times

Case 7: When the applied load is 20N, frequency is 50Hz and experiment run for 10 minutes. The graph between co-efficient and time is shown below in fig. 5.7.

.

Fig. 5.7: Graph of COF versus time

Case 8: When the applied load is 15N, frequency is 50Hz and experiment run for 10 minutes. The graph between frictional force and time is shown below in fig. 5.8.

Fig. 5.8: Graph of FF versus Time

Case 9: When the applied load is 15N, frequency is 50Hz and experiment run for 10 minutes. The graph between temperature and time is shown below in fig. 5.9.

Fig. 5.9: Graph of Temperature versus Times

Case 10: When the applied load is 25N, frequency is 50Hz and experiment run for 10 minutes. The graph between co-efficient of friction and time is shown below in fig. 5.10.

Fig. 5.10: Graph of COF versus time

Case 11: When the applied load is 25N, frequency is 50Hz and experiment run for 10 minutes. The graph between frictional force and time is shown below in fig. 5.11.

Fig. 5.11: Graph of FF versus Time

Case 12: When the applied load is 25N, frequency is 50Hz and experiment run for 10 minutes. The graph between temperature and time is shown below in fig. 5.12.

Fig. 5.12: Graph of Temperature versus Times

5.3 Optical microscopic images

An optical microscope is used to view the microscopic structure of the Aluminium alloy. The sample is magnified in the range of 100x, 200x, 500x and 1000x to view the structure of copper and nickel. The structure of copper and nickel is clearly shown in microscopic images. The crystals of copper and nickel are perfectly blended in Aluminium and the grain boundaries are revealed. The presence of copper particle helps in increasing the thermal conductivity of the specimen and subsequent aging with an increase in strength and hardness and a decrease in hardness. Addition of magnesium increases the strength of aluminium without decreasing its ductility. Corrosion resistance and weldablitiy are good. The addition of nickel increases strength but reduces its ductility but on adding it with copper it improves hardness and strength at high temperatures and it also reduces coefficient of expansion. The grain boundaries of copper and nickel are distinctively seen. Voids are also present which shows the imperfectness in casting process and can lead to failure of material. The optically taken images of specimen are categorised in the order of their magnification and below is a image of magnification 100x and subsequently 200x, 500x, and 1000x images are also there.

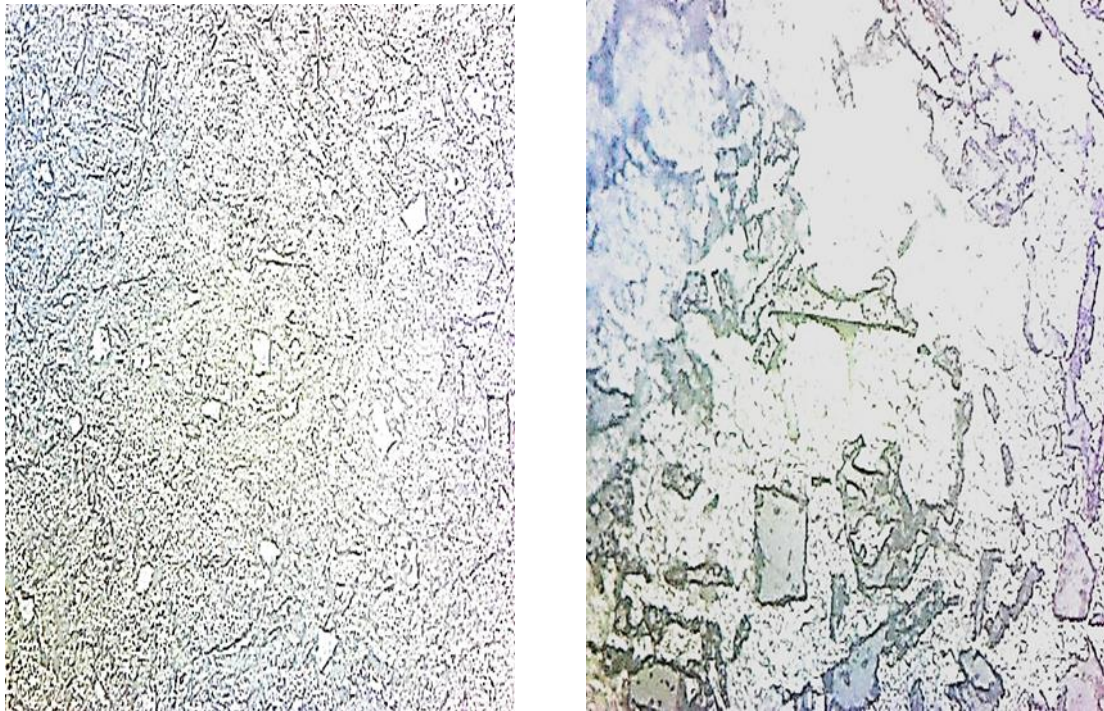**Fig.** 5.13: 100 times magnified image of specimen [source: DTU]

Fig 5.14: 200 and 500 time Magnified image of specimen [source, DTU]

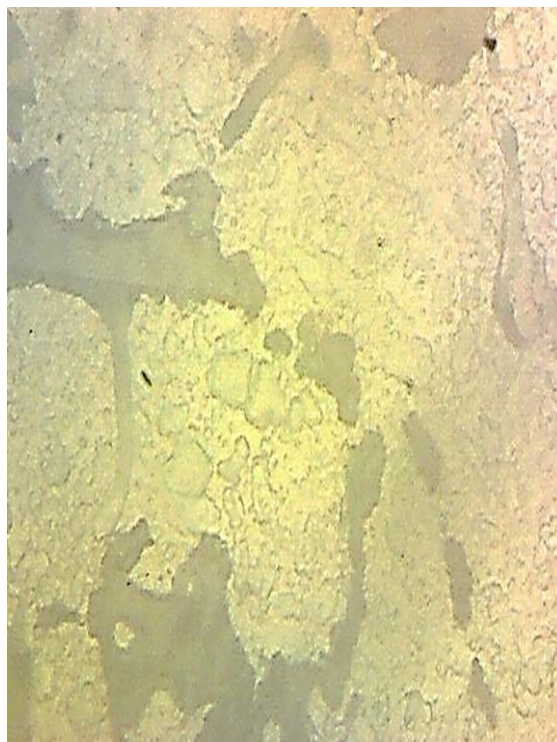**Fig.** 5.15: 1000 time magnified image of specimen [source: DTU]

5.4 Scanning Electron microscopy

Scanning electron microscopy reveals the grain structure as well as the composition in the material. The results of SEM shows the presence of carbon, silicon, magnesium, aluminium, nickel. The presence of carbon is due to the polishing on emery paper, emery paper consist of carbon and iron, the carbon of emery paper got embedded in the surface of specimen. Thus on testing the specimen the traces of carbon is found. The presence of silicon is due the manufacturing technique, during casting the silicon present in the casting sand mixes with the molten sample and thus there is presence of silicon in specimen. The images shows the flakes of magnesium, aluminium, nickel and copper. Grains of copper are clearly embedded in the surface of specimen with other grains of nickel and magnesium. The energy dispersive X-ray spectroscopy confirms the presence of copper, nickel, magnesium in aluminium. The original by weight composition varies with the values taken by EDAX because at certain points the mixing of material varies thus there rise a variation in composition at different points of the sample.
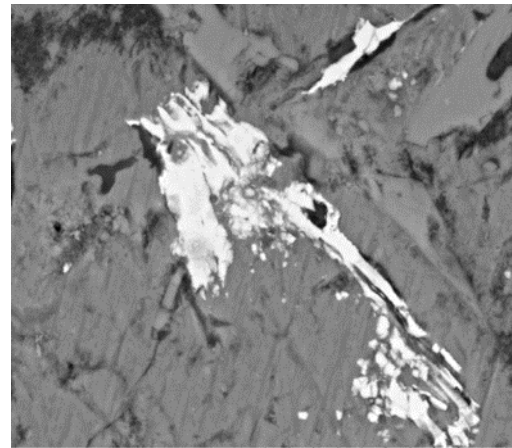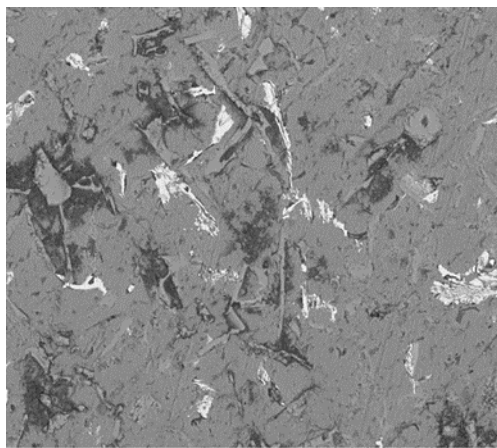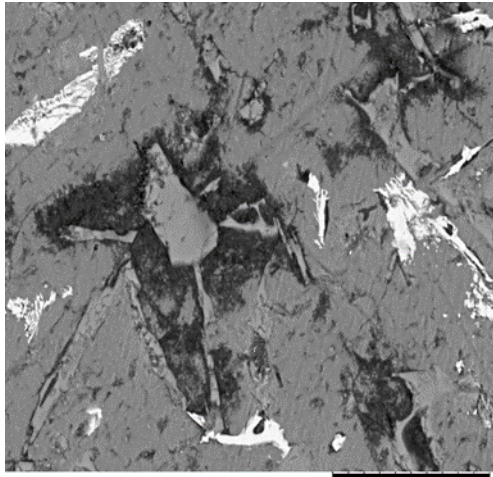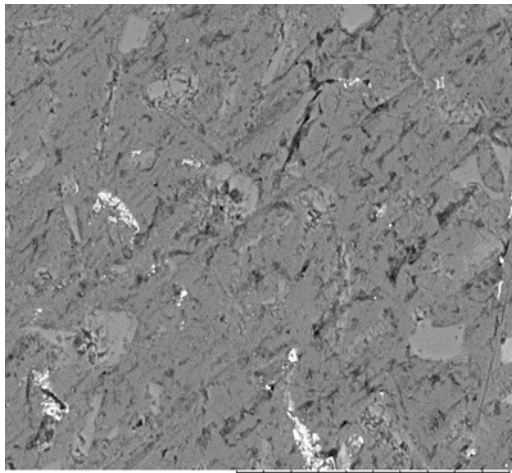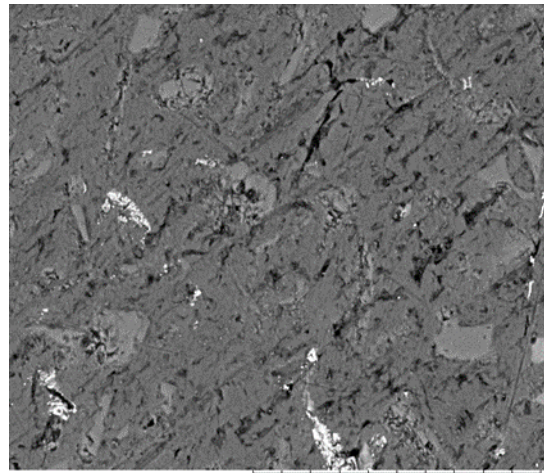
TM3000_3527   2019/07/24 11:13 H   D6.2 x1.2k   50 um
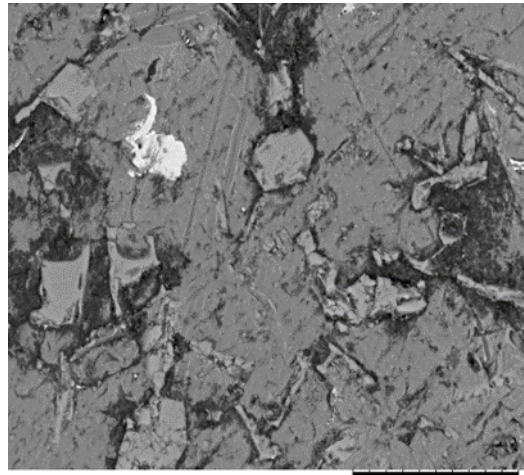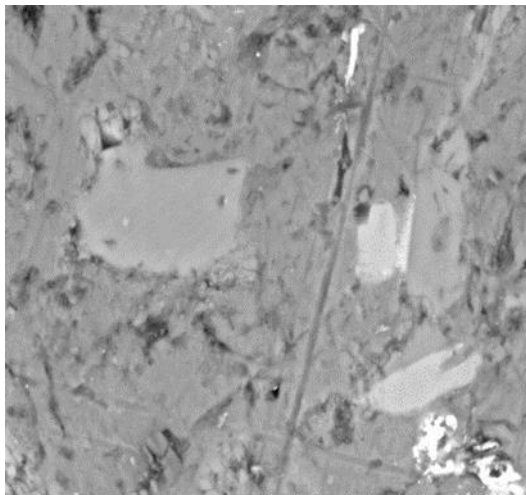

TM3000_3528   2019/07/24 11:15 H   D6.2 x1.2k   50 um
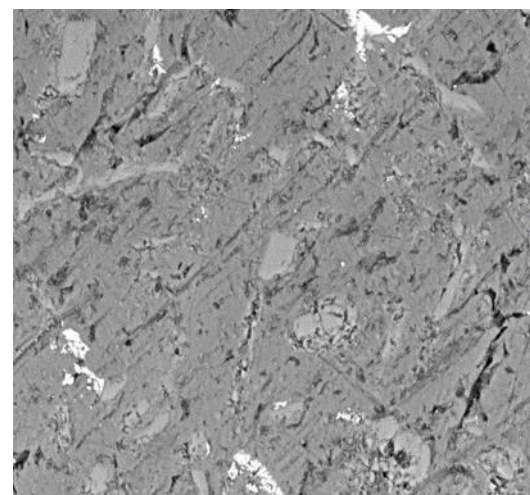

TM3000_3529   2019/07/24 11:16 H   D6.2 x1.0k   100 um

TM3000_3530   2019/07/24 11:16 H   D6.2 x1.0k   100 um

TM3000_3531   2019/07/24 11:19 H   D6.1 x3.0k   30 um

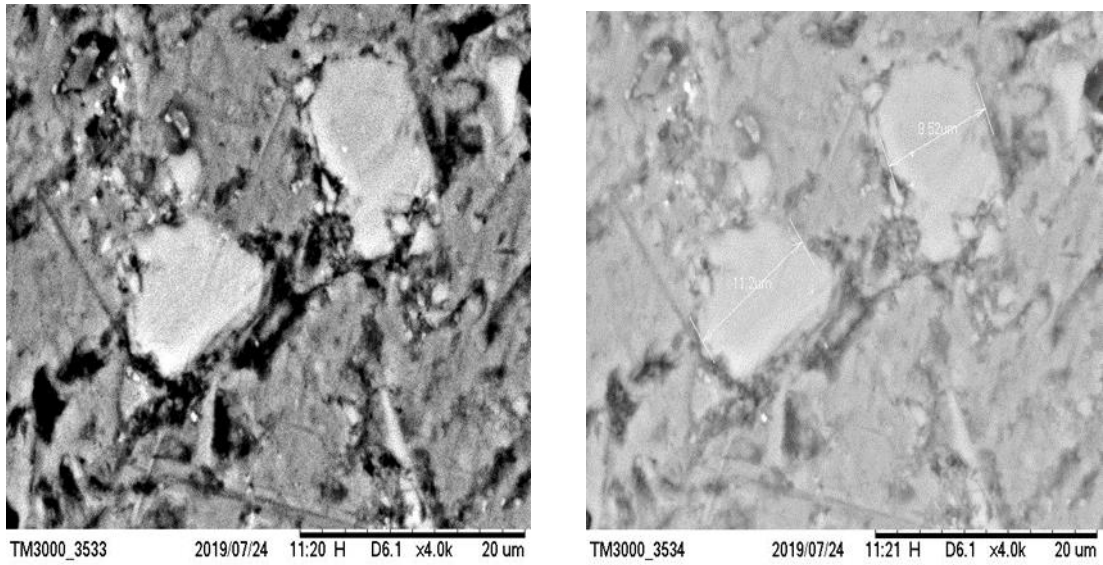
TM3000_3535   2019/07/24 11:23 H   D6.1 x1.2k   50 um

47

Fig. 5.16: SEM images of specimen [source: IIT, Delhi]

Spectrum details

Project New project   Spectrum name   Spectrum 1
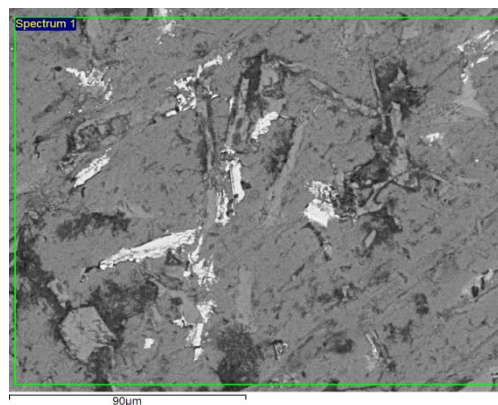
Electron Image

Image Width: 189.6 μm

Fig. 5.17: Electron image [source: IIT, Delhi]

Acquisition conditions

Acquisition time (s) 60.3   Process time 4
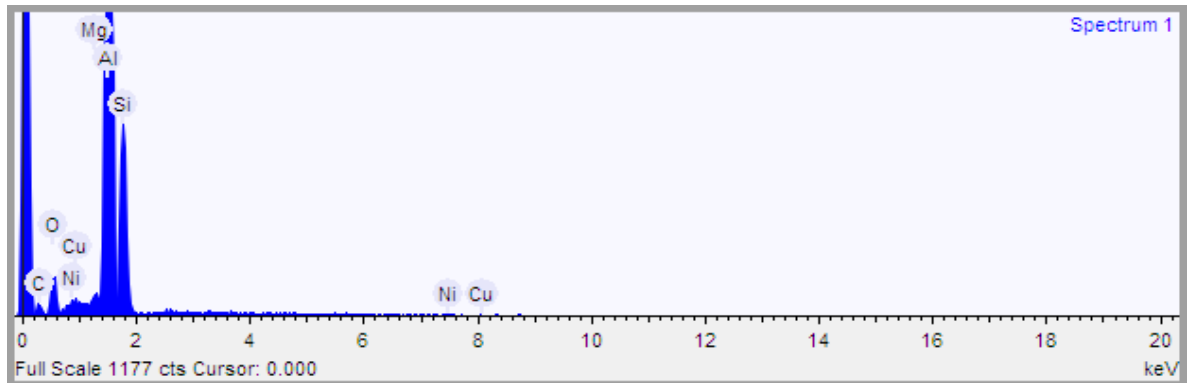
Accelerating voltage (kV)   15.0

Fig. 5.18: Graph of element compostion concentration [source: IIT, Delhi]

Quantification Settings

Quantification method   All elements (normalised)

Coating element   none

Summary results

Table 5.3: Composition of Specimen

Element	Weight %	Weight % σ	Atomic %
Carbon	16.091	1.426	28.429
Magnesium	0.421	0.100	0.367
Aluminum	52.936	1.032	41.633
Nickel	0.980	0.311	0.354
Copper	0.473	0.334	0.158

5.5 Hardness tester

The hardness testing is done on Fischer hardness tester, the value of hardness is taken from it. The indenter is allowed to indent for a period of about 20 seconds and a force of 300.00 mN is applied. Total a set of five readings have been taken and are compared. One of the reading is improper showing the casting defect present in the specimen. The martensitic hardness value shows a min of reading of 876.1 N/mm² and a max reading of 1413.5 N/mm² where as the Vickers hardness test shows the max and min value of 161.5 and 97.0 Mpa. The value of modulus of hardness shows a max and min value of 117.3 GPa and 91.6 GPa.
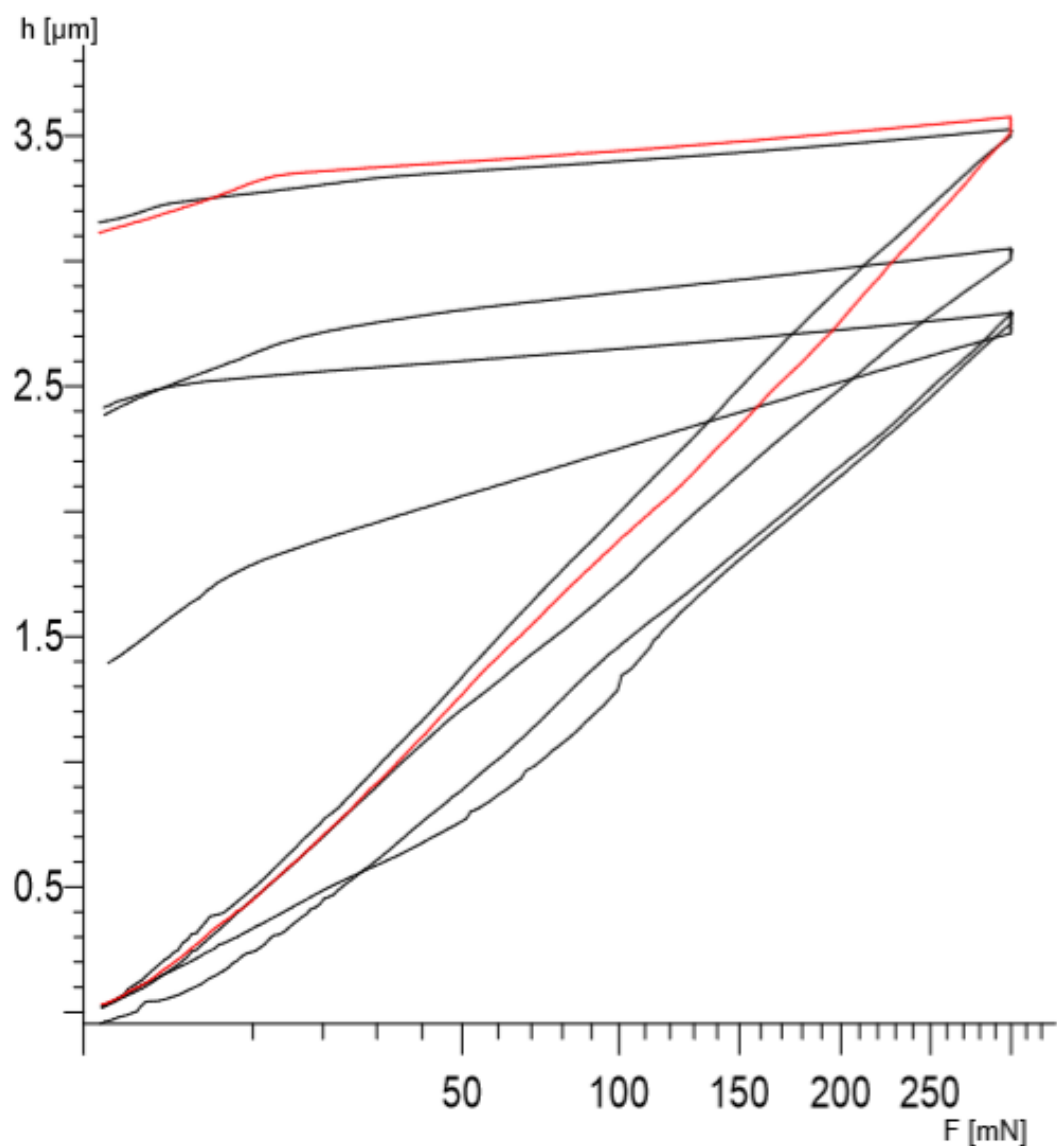

Fig. 5.17: Graph of Force versus Indentation

5.6 Design of Experiment (DOE)

DOE is applied to study the relation of various factors like load, temperature and time on the wear properties of specimen. The results signifies that these factors clearly have direct effect on the wear property of specimen. In this experiment 9 sets of reading have been taken for wear and studied. The controlling factors are selected with the help of taguchi optimization technique and a table is formed from these controlling factors.

Taguchi method calculated the value of mean and standard deviation and plotted the graph for both of them. The graph shows the mean and standard deviation of wear rate line from load, temp and time. The wear first starts increasing due to absence of non-formation of lubricant boundary layer but when there is a formation of lubricant film the value of wear starts decreasing down. The table is then analysed and the graphs have been plotted with the help of this table.

Table 5.4: Optimized value of mean and standard deviation for wear

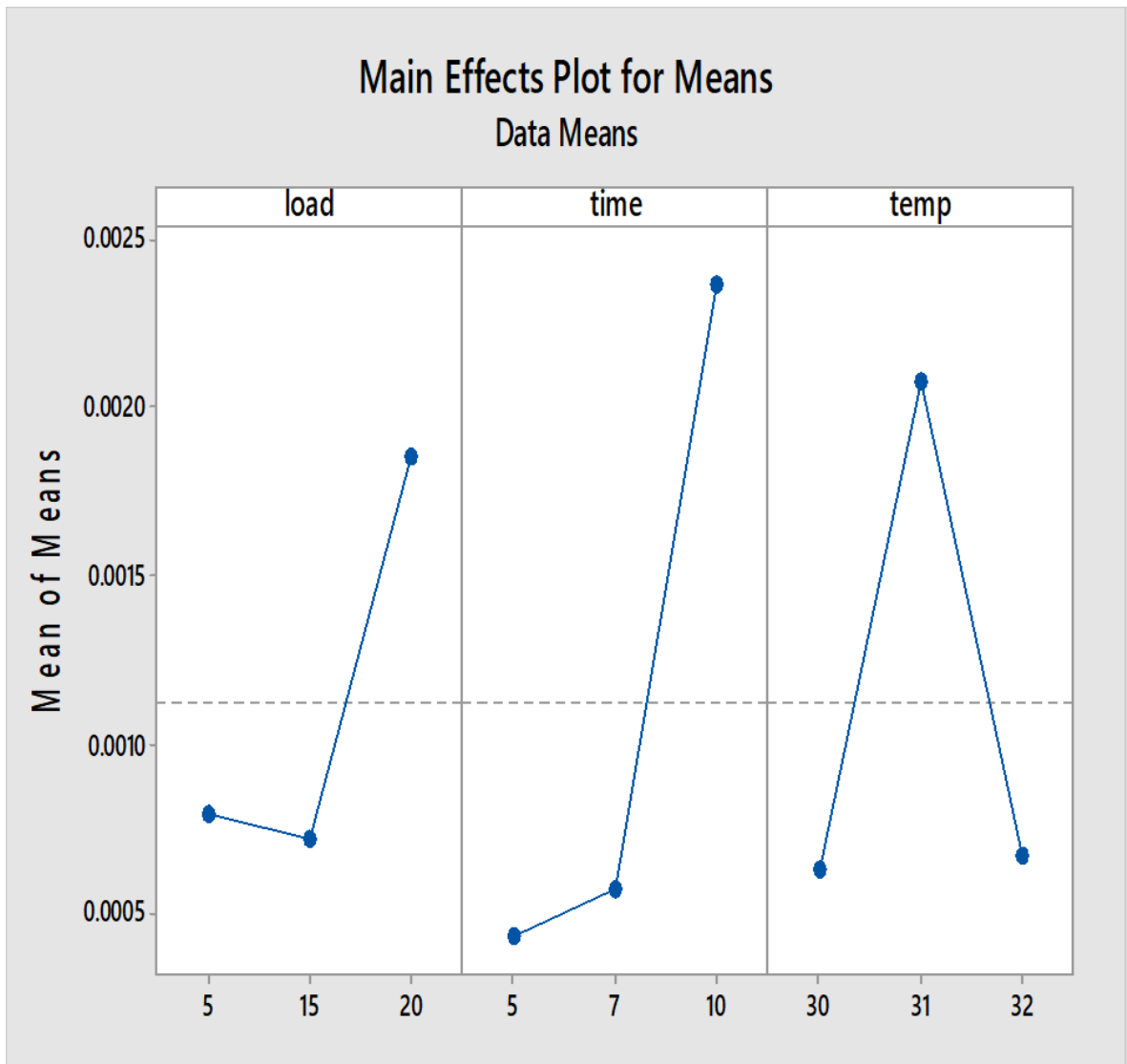| S.No.	LOAD	TIME	TEMP.	WEAR(in gms)	SNRA1	MEAN1
1	5	5	30	0.00055	65.1927	0.00055
2	5	7	31	0.00073	62.7335	0.00073
3	5	10	32	0.00110	59.1721	0.00110
4	15	5	31	0.00050	66.0206	0.00050
5	15	7	32	0.00066	63.6091	0.00066
6	15	10	30	0.00100	60.0000	0.00100
7	20	5	32	0.00025	72.0412	0.00025
8	20	7	30	0.00033	69.6297	0.00033
9	20	10	31	0.00500	46.0206	0.00500

Fig. 5.18: Graph of Mean versus Load, Time, Temperature

On increasing the load the value of wear starts increasing because higher the load the higher the value of frictional forces developed in it thus causes increases friction. With passage of time the value of wear starts increasing, the more time the specimen is in contact with other reciprocating specimen the wear will be more. Thus wear is dependent on the time of engagement of the specimens. The value of wear first increases with temperature but then decrease with increases in temperature because the lubricant may start working well with elevated temperatures, the fluidity of lubricant increases with increases in temperature thus the lubricating properties enhanced with increasing temperature.
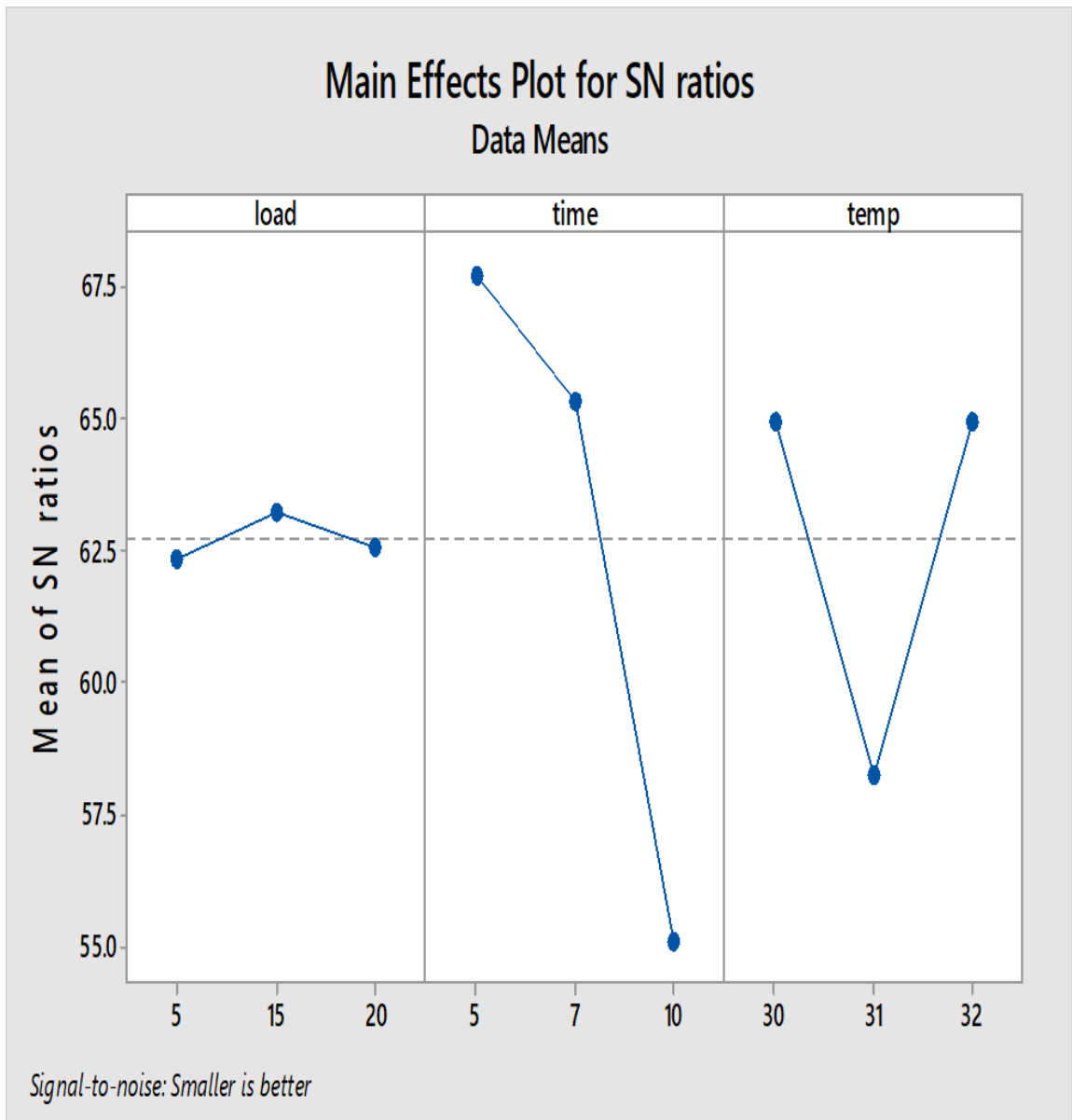
Fig. 5.19: Graph of standard deviation versus Load, Time, Temperature

The standard deviation of wear form its mean value under the influencing factors like load, temperature and time is shown in this graph. The value of wear doesn't show much variation with load but it show much deviation with time and temperature. Thus we can conclude that time and temperature has much more effect on wear property than load.

CHAPTER 6: CONCLUSION AND FUTURE SCOPE

Conclusion

This dissertation work is done to study the tribological performance of modified piston with cylinder of hermetically sealed compressor. The results shows average value of wear which are better than the previous values that are found with the existing material of the piston. Thus this material can be used for manufacturing of piston of hermetically sealed compressor. The optical microscopic images show the internal geometry of material. The grain structure of copper and nickel embedded in Aluminium is shown. The optical images shows the presence of voids which shows some drawbacks in casting process. CNC machining can produce highly precised pistons with better surface finish.

Design of experiment is applied to get the optimize results for wear under the factors such as load, time and temperature various graphs have been plotted which shows the wear pattern. The value of wear increases with increase in load and time while in case of temperature is first increase and then decrease with time due to formation of better lubricant film. The activity of lubricant increases at certain temperature thus value of wear decreases with increase in temperature.

The hardness of the material is improved from the existing material due to presence of copper and nickel. Presence of nickel with copper improves the performance of the material at elevated temperatures while the ductility is decreased. The welding properties of material are also enhanced.

Future Scope

Compressor being the heart of air-conditioning as well as refrigerating appliances there is a lot of scope for future research. In this experiment consideration is only on piston material whereas improvements can also be done on cylinder material.

Lubricant plays a major role in controlling the wear properties as well as distributing the temperature in the compressor, thus a wide scope is open for research in the field of the lubrication.

REFRENCES

[1] Lusha Tian, Yongchun Guo, Jianping Li, Jianli Wang, Hongbo Duan, Feng Xia, Minxian Liang, "Elevated re-aging of a piston aluminium alloy and effect on the microstructure and mechanical properties," in Material science and engineering A 738, 2018, pp. 375-379.

[2] Love Kerni, Ankush Raina, Mir Irfan Ul Haq, "Performance evaluation of aluminium alloys for piston and cylinder applications," in Materials Today Proceedings 5, 2018, pp. 18170–18175.

[3] Zhimin Yao, Kunsheng Hu, Rong Li, "Enhanced high-temperature thermal fatigue property of aluminium alloy piston with Nano PYSZ thermal barrier coatings," in Journal of Alloys and Compounds 790, 2019, pp. 466-479.

[4] W.T. Riad, B.S. Hussain, H.M. Shalaby, "Cracking of aluminium cast pistons of fuel gas reciprocating compressors," in Engineering Failure Analysis 17, 2010, pp. 440–446.

[5] J.D.B. De Mello, R. Binder, N.G. Demas, A.A. Polycarpou, "Effect of the actual environment present in hermetic compressors on the tribological behaviour of a Si-rich multifunctional DLC coating," in Wear 267, 2009, pp. 907–915.

[6] Seung Min Yeo, Andreas A. Polycarpou, "Tribological performance of PTFE- and PEEK-based coatings under oil-less compressor conditions," in Wear 296, 2012, pp. 638–647.

[7] B. Raja, S. Joseph Sekhar, D. Mohan Lal, A. Kalanidhi, "A numerical model for thermal mapping in a hermetically sealed reciprocating refrigerant compressor," in International Journal of Refrigeration 26, 2003, pp. 652–658.

[8] Miguel B. Demay, Carlos A, Flesch, André P. Rosa, "Indirect measurement of hermetic compressor speed through externally-measurable quantities," in International journal of refrigeration 34, 2011, pp. 1268-1275.

[9] Sun Zhe, Gu Jiangping, Jin Huaqiang, Huang Yuejin, Shen Xi, "An investigation on speed measurement method of hermetic compressor based on current fluctuation," in International journal of refrigeration 88, 2018, pp. 211-220.

[10] C.D. Perez-Segarra, J. Rigola, M. Soria, A. Oliva, "Detailed thermodynamic characterization of hermetic reciprocating compressors," in International Journal of Refrigeration 28, 2005, pp. 579–593.

[11] N.P. Garland, M. Hadfield, "Environmental implications of hydrocarbon refrigerants applied to the hermetic compressor," in Materials and Design 26, 2005, pp. 578–586.

[12] Sathuramalingam Pillay Darminesha, Nor Azwadi Che Sidika, G. Najafic, Rizalman Mamatd, Tan Lit Kenb, Yutaka Asako, **"**Recent development on biodegradable nano lubricant," in International communication in heat and mass transfer 86, 2017, pp. 159-165.

[13] C. Ciantar, M. Hadfield, A. Swallow, A. Smith, "The influence of POE and PVE lubricant blends within hermetic refrigerating compressors operating with HFC-134a refrigerant," in Wear 241, 2000, pp. 53–64.